

Interaction of Glucagon-Like Peptide 1 and Its Analogues with Amyloid- β Peptide Affects Its Fibrillation and Cytotoxicity

[Ekaterina A. Litus](#)*, [Marina P. Shevelyova](#), [Alisa A. Vologzhannikova](#), [Evgenia I. Deryusheva](#), [Alina V. Chaplygina](#), [Victoria A. Rastrygina](#), [Andrey V. Machulin](#), Valeria D. Alikova, Aliya A. Nazipova, [Maria E. Permyakova](#), [Victor V. Dotsenko](#), [Sergei E. Permyakov](#), [Ekaterina L. Nemashkalova](#)

Posted Date: 24 April 2025

doi: 10.20944/preprints202504.2038.v1

Keywords: diabetes mellitus; glucagon-like peptide-1; liraglutide; exenatide; semaglutide; Alzheimer's disease; amyloid- β peptide; A β fibrillation; cytotoxicity; bio-layer interferometry; surface plasmon resonance; dynamic light scattering; electron microscopy; molecular docking



Preprints.org is a free multidisciplinary platform providing preprint service that is dedicated to making early versions of research outputs permanently available and citable. Preprints posted at Preprints.org appear in Web of Science, Crossref, Google Scholar, Scilit, Europe PMC.

Copyright: This open access article is published under a Creative Commons CC BY 4.0 license, which permit the free download, distribution, and reuse, provided that the author and preprint are cited in any reuse.

Article

Interaction of Glucagon-Like Peptide 1 and Its Analogues with Amyloid- β Peptide Affects Its Fibrillation and Cytotoxicity

Ekaterina A. Litus ^{1,*}, Marina P. Shevelyova ^{1,†}, Alisa A. Vologzhannikova ¹, Evgenia I. Deryusheva ¹, Alina V. Chaplygina ¹, Victoria A. Rastrygina ¹, Andrey V. Machulin ², Valeria D. Alikova ¹, Aliya A. Nazipova ¹, Maria E. Permyakova ¹, Victor V. Dotsenko ³, Sergei E. Permyakov ¹ and Ekaterina L. Nemashkalova ¹

¹ Institute for Biological Instrumentation, Pushchino Scientific Center for Biological Research of the Russian Academy of Sciences, Pushchino, Moscow Region 142290, Russia

² Skryabin Institute of Biochemistry and Physiology of Microorganisms, Pushchino Scientific Center for Biological Research of the Russian Academy of Sciences, Pushchino, Moscow Region 142290, Russia

³ Department of Organic Chemistry and Technologies, Kuban State University, 149 Stavropolskaya St., 350040 Krasnodar, Russia

* Correspondence: ealitus@gmail.com; Tel.: +7-(495)-143-7741; Fax: +7-(4967)-33-05-22

† These authors contributed equally to this work.

Abstract: Clinical data, as well as animal and cell studies indicate that certain some antidiabetic drugs, including glucagon-like peptide 1 receptor agonists (GLP-1RAs), exert therapeutic effects in Alzheimer's disease (AD) by modulating amyloid- β peptide ($A\beta$) metabolism. Meanwhile, the direct interactions of GLP-1RAs with $A\beta$ and their functional consequences remain unexplored. In this study, the interactions between monomeric $A\beta_{40}/A\beta_{42}$ of GLP-1(7-37) and its several analogues (semaglutide (Sema), liraglutide (Lira), exenatide (Exen)) were studied using biolayer interferometry and surface plasmon resonance spectroscopy. Quaternary structure of the GLP-1RAs was investigated by dynamic light scattering. The effects of GLP-1RAs on $A\beta$ fibrillation were assessed by Thioflavin T assay and electron microscopy. The impact of GLP-1RAs on $A\beta$ cytotoxicity was evaluated via the MTT assay. Monomeric $A\beta_{40}$ and $A\beta_{42}$ directly bind to GLP-1(7-37), Sema, Lira, Exen, with highest affinity for Lira (the lowest estimates of equilibrium dissociation constants are 42-60 nM). The GLP-1RAs are prone to oligomerization, which may affect their binding to $A\beta$. GLP-1(7-37) and Exen inhibit $A\beta_{40}$ fibrillation, whereas Sema promoted it. The GLP-1 analogues decreased $A\beta$ cytotoxicity towards SH-SY5Y cells, while GLP-1(7-37) enhanced the $A\beta_{40}$ cytotoxicity without affecting the cytotoxic effect of $A\beta_{42}$. Overall, the GLP-1RAs interact with $A\beta$ and differentially modulate its fibrillation and cytotoxicity, suggesting the need for further studies of our observed effects in vivo.

Keywords: diabetes mellitus; glucagon-like peptide-1; liraglutide; exenatide; semaglutide; Alzheimer's disease; amyloid- β peptide ($A\beta$); protein-protein interaction; $A\beta$ fibrillation; $A\beta$ cytotoxicity

1. Introduction

Alzheimer's disease (AD) is a neurodegenerative disease characterized by a gradual decline in cognitive abilities and memory impairment, which significantly complicates social and professional activities. Worldwide, approximately 416 million individuals are affected by AD dementia, prodromal AD, or preclinical AD, accounting for 22% of the population aged 50 years and older [1]. To date, U.S. Food and Drug Administration (FDA) has approved nine drugs for treatment of AD, of which only three (aducanumab, lecanemab, donanemab) are used for pathogenetic therapy and

target the reduction of amyloid- β peptide ($A\beta$) deposits [2,3]. At the same time, the use of these drugs is associated with side effects, such as brain edema and microhemorrhages [4]. $A\beta$ plays a central role in the AD pathology [5]. It is derived from a transmembrane amyloid precursor protein (APP), through sequential proteolytic cleavage by β -secretase and γ -secretase [6]. The predominant forms of $A\beta$ are the peptides comprising of 38, 40 or 42 residues, $A\beta_{38}$, $A\beta_{40}$ and $A\beta_{42}$, respectively [7,8]. Monomeric $A\beta$ is intrinsically disordered and therefore prone to aggregation with formation of short fibrillar oligomers, most cytotoxic globular nonfibrillar oligomers, and mature amyloid fibrils [9].

Epidemiological data indicate a strong link between AD and diabetes mellitus (DM): patients with diabetes have a 65% increased risk of developing AD [10,11]. DM is a severe chronic disease that has a serious impact on the life and well-being of individuals, families and society. Globally, at least 529 million people suffer from diabetes [12]. Type 2 diabetes mellitus (DM2) is the most prevalent form of DM (90% of all cases), characterized by high blood glucose levels (hyperglycemia) and insulin resistance [13]. The last one, along with neuroinflammation, oxidative stress, increased levels of advanced glycosylation end products, mitochondrial dysfunction, metabolic syndrome, and the accumulation of $A\beta$ and tau protein in the brain, are common features of AD and DM2 (reviewed in [14]). Therefore, type 3 diabetes, which manifests as insulin resistance in brain tissue, affects cognitive function and contributes to AD progression, has recently been proposed as a brain-specific type of DM [15].

Clinical studies in patients with mild cognitive impairment and AD have demonstrated that administration of certain antidiabetic medications, including intranasal insulin, metformin, incretins, and thiazolidinediones, can improve cognition and memory (reviewed in [16]). Incretins (glucagon-like peptide 1 (GLP-1) and gastric inhibitory peptide) are gut hormones that are secreted after nutrient intake and act on the pancreatic β -cells to enhance glucose-stimulated insulin secretion [17]. Incretin-based therapy (including truncated GLP-1 and its derivatives) is playing an increasingly important role in treatment of DM2 due to its efficacy and safety [18,19].

The N-terminally truncated forms of GLP-1, GLP-1(7-36)/(7-37), secreted from intestinal L cells [20], control meal-related glycemic excursions by augmentation of insulin expression and secretion and inhibition of glucagon release (reviewed in [21]). Some population of neurons in the *nucleus tractus solitarius* of the brainstem can also express GLP-1 [22,23]. GLP-1 can cross the blood-brain barrier (BBB) [24] and acts through GLP-1 receptor, GLP-1R, which is expressed in several brain regions, including the hypothalamus, cerebral cortex, *amygdala*, *hippocampus*, *caudate putamen*, and *globus pallidum* [25]. GLP-1 signaling is important for cognition, and preclinical studies evidence neuroprotective action of GLP-1 [26,27]. Murine GLP-1R contributes to control of synaptic plasticity and memory formation [28]. GLP-1R-deficient mice have a learning-deficient phenotype which can be rescued through hippocampal GLP1R gene transfer, while the rats overexpressing GLP-1R in the hippocampus show improved memory and learning abilities [29]. GLP-1(7-36) has been shown to reduce $A\beta$ levels in the mouse brain in vivo and to decrease levels of APP in cultured neuronal cells [30]. Similarly, GLP-1(7-36) protects cultured hippocampal neurons against $A\beta$ /iron-induced death [30], while mutated GLP-1 rescues SH-SY5Y cells from $A\beta_{42}$ -induced apoptosis [31].

GLP-1 is efficiently inactivated by dipeptidyl peptidase-4 (DPP-4) and neutral endopeptidase 24.11, resulting in a plasma half-life of GLP-1 of approximately 1.5-5 minutes [32–34]. To overcome this limitation, DPP-4 inhibitors and long-acting GLP-1R agonists (GLP-1RAs) resistant to proteolysis by DPP-4 have been developed for clinical use (reviewed in [32,35]): Exenatide (Exen), Liraglutide (Lira), Semaglutide (Sema), etc.

Exen (trade name Byetta) consists of 39 amino acid residues with 53% homology to human GLP-1(7-37) (Figures 1A, 1C), and is resistant to DPP-4-mediated inactivation [36]. Exen decreases $A\beta$ toxicity and oxidative stress in primary neuronal cultures and SH-SY5Y cells, interferes with the development of cognitive impairments and significantly reduces brain levels of APP and $A\beta$ in animal AD models [37–40]. Reduced $A\beta$ accumulation in response to Exen has been shown in both mouse and worm AD models [40,41]. Evaluation of the Exen's effect in patients with moderate Parkinson's disease showed sustained improvements in cognitive and motor measures [42].

Meanwhile, a pilot study of Exen in AD did not reveal significant differences in clinical, cognitive, or biomarker outcomes compared with placebo, except for a reduction in A β 2 levels in extracellular vesicles [43].

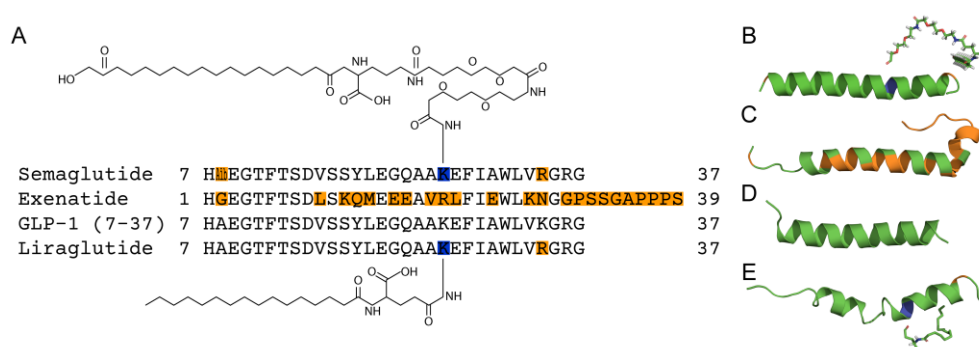


Figure 1. The alignment of amino acid sequences (panel A) and model structures of the GLP-1RAs (B-E): Sema (B: based on PDB entry 7KI0, EM, chain E), Exen PDB ID 1JRJ, NMR, chain A, model 1), GLP-1(7-37) (D: PDB ID 3IOL, X-ray, chain B) and Lira (E: PDB ID 4APD, NMR, chains A, B, model 1). The amino acid residues that differ from those in GLP-1 are marked in orange (Aib, 2-aminoisobutyric acid). The lysine residues of Sema and Lira modified by the linkers with fatty acids are highlighted in blue. The numbering of the residues is according to the PDB entries.

Another long-acting GLP-1 derivative, Lira (brand names Victoza and Saxenda), differs from GLP-1(7-37) by K34R substitution and palmitic acid attached to K26 residue through a glutamic acid spacer (Figures 1A, 1E). The attached fatty acid chain favors binding to serum albumin thereby slowing the clearance of Lira [44,45]. Lira has been shown to alleviate neuronal insulin resistance and to reduce A β formation and tau hyperphosphorylation in SH-SY5Y cells [46]. Tests of Lira in APP/PS1 AD mice showed that it crosses the BBB, prevents memory loss and hippocampal deterioration, increases the number of young neurons in the dentate gyrus, and reduces neuronal inflammation, A β oligomer, APP levels, and A β plaque formation [47–49]. In clinical trials involving AD patients, Lira was found to prevent the decline of brain glucose metabolism, however, it did not significantly affect A β accumulation or cognition [50]. Functional magnetic resonance imaging revealed significant improvement in intrinsic connectivity in the default mode network in the group of persons at risk for AD taking Lira, but without detectable cognitive differences between the study groups [51].

Sema (trade names Ozempic, Wegovy, etc.) is a prolonged-release form of Lira with increased affinity for HSA, suitable for once-weekly administration [52]. Compared to Lira, Sema contains 2-aminoisobutyric acid at position 2 (prevents breakdown by DPP-4) and differs in structure of the fatty acid chain (C18 di-acid chain) and its linker (Figures 1A, 1B). Sema protects SH-SY5Y cells from A β 25-35 by enhancement of autophagy and inhibition of apoptosis [53]. The neuroprotective and anti-inflammatory properties of Sema were shown in a rat model of stroke [54]. Recent studies using human AD brain organoids have shown that Sema decreases levels of A β and phosphorylated tau levels. Additionally, in APP/PS1 transgenic mice, Sema improves cognitive performance, particularly learning and memory, and reduces amyloid plaque [55]. Oral form of Sema is currently being tested in patients with early AD in phase 3 clinical trials (NCT04777396 and NCT04777409) [56,57].

Despite encouraging clinical data, animal and cellular studies on the role of GLP-1 and its analogues in AD progression, information on their direct interaction with A β is lacking. To fill this gap, in the present study we probe the interaction of several GLP-1RAs with monomeric A β 40/42 using biolayer interferometry (BLI) and surface plasmon resonance (SPR) spectroscopy. Furthermore, we assess the effects of, of the GLP-1RAs on A β fibrillation and A β cytotoxicity towards SH-SY5Y cells.

2. Results

2.1. Interaction of GLP-1RAs with Monomeric A β

A β 40/A β 42 was immobilized on the surface of BLI sensor by amine coupling using EDAC/sulfo-NHS, followed by removal of the non-covalently bound A β molecules with 0.5% SDS solution, which ensured monomeric state of A β . Passage over the sensor of 4–50 μ M solutions of GLP-1(7–37), Exen, Lira and Sema in the buffer simulating conditions of the extracellular space results in the concentration-dependent sensograms characteristic of association/dissociation phases (Figure 2). Some of the resulting kinetic curves were successfully fitted using either a single binding site model (1) or a heterogeneous ligand scheme (2) (Figure 2). The resulting parameters of the GLP-1RA – A β interactions are summarized in Table 1. Meanwhile, some of the kinetic data are not consistent with these interaction models. Nevertheless, the clear signs of these interactions evidence that their equilibrium dissociation constants, K_D , reach the level of the analyte concentrations used in the BLI experiments, i.e., 25–50 μ M for GLP-1(7–37) and 4–15 μ M for Exen. The highest affinity for A β 40/A β 42 is observed for Lira with K_D values of 42–60 nM at protein concentrations of 5–10 μ M (Table 1). Sema is 2.4–2.6 orders of magnitude less specific to A β 40/A β 42 (K_D values of 11–22 μ M) at protein concentrations of 17–38 μ M.

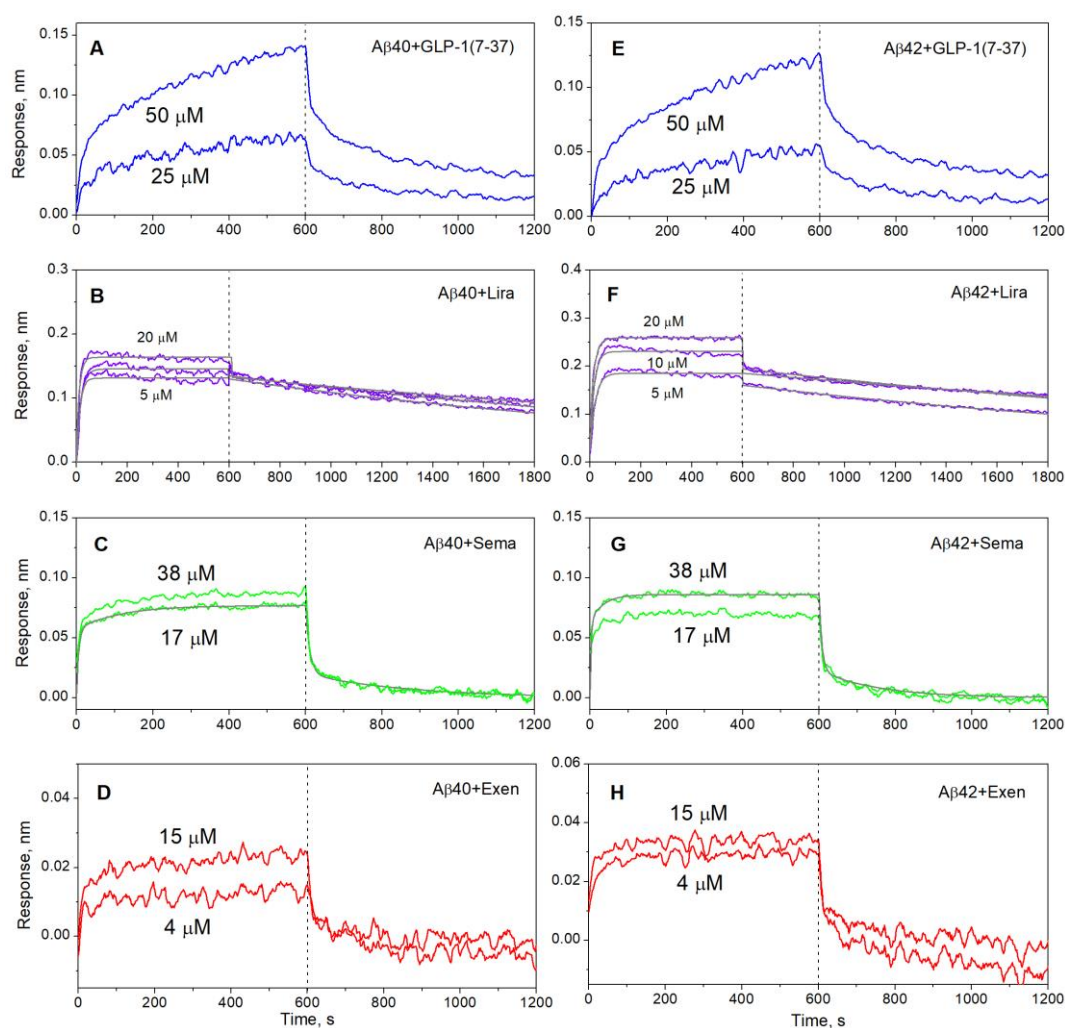


Figure 2. Kinetics of GLP-1(7–37) (blue), Exen (red), Lira (violet) and Sema (green) interaction with monomeric A β 40 (panels A–D) or A β 42 (E–H) immobilized on sensor surface by amine coupling, monitored using BLI at 25°C (20 mM HEPES-KOH/Tris-HCl, 140 mM NaCl, 4.9 mM KCl, 2.5 mM CaCl₂, 1 mM MgCl₂, pH 7.4). The analyte concentrations are indicated nearby the sensograms. The black curves are theoretical, calculated

according to the single binding site scheme (1) or heterogeneous ligand model (2) (see Table 1 for the fitting parameters).

Table 1. Parameters of the interaction between monomeric Aβ40/Aβ42 and the GLP-1RAs at 25°C, estimated from the BLI data shown in Figure 2 using either single binding site model (1) or heterogeneous ligand scheme (2).

	$[Lira], \mu M$	$k_a, M^{-1}s^{-1}$	k_d, s^{-1}	K_D, M	$k_a, M^{-1}s^{-1}$	k_d, s^{-1}	K_D, M
		$A\beta 40$			$A\beta 42$		
$Lira$	20	$(8.4 \pm 2.8) \times 10^3$	$(9.0 \pm 0.4) \times 10^{-4}$	$(1.1 \pm 0.4) \times 10^{-7}$	$(5.7 \pm 1.1) \times 10^3$	$(6.0 \pm 0.2) \times 10^{-4}$	$(1.1 \pm 0.2) \times 10^{-7}$
	10	$(7.3 \pm 0.4) \times 10^3$	$(3.46 \pm 0.07) \times 10^{-4}$	$(4.8 \pm 0.3) \times 10^{-8}$	$(8.0 \pm 0.7) \times 10^3$	$(4.82 \pm 0.12) \times 10^{-4}$	$(6.0 \pm 0.2) \times 10^{-8}$
	5	$(1.34 \pm 0.09) \times 10^4$	$(5.56 \pm 0.11) \times 10^{-4}$	$(4.2 \pm 0.3) \times 10^{-8}$	$(1.21 \pm 0.08) \times 10^4$	$(5.40 \pm 0.12) \times 10^{-4}$	$(4.5 \pm 0.3) \times 10^{-8}$
	$[Sema], \mu M$	$k_{a1}, M^{-1}s^{-1}$	k_{d1}, s^{-1}	K_{D1}, M	$k_{a2}, M^{-1}s^{-1}$	k_{d2}, s^{-1}	K_{D2}, M
		$A\beta 40$					
$Sema_a$	17	310±52	$(3.7 \pm 0.2) \times 10^{-3}$	$(1.2 \pm 0.2) \times 10^{-5}$	$(5.7 \pm 1.1) \times 10^3$	$(9.1 \pm 0.6) \times 10^{-2}$	$(1.6 \pm 0.3) \times 10^{-5}$
		$A\beta 42$					
	38	582±104	$(6.4 \pm 0.6) \times 10^{-3}$	$(1.1 \pm 0.2) \times 10^{-5}$	$(6.1 \pm 2.7) \times 10^3$	$(1.34 \pm 0.15) \times 10^{-1}$	$(2.2 \pm 1.0) \times 10^{-5}$

The analogous examination of Aβ40/Aβ42 affinity for the GLP-1RAs using SPR spectroscopy and Aβ as a ligand (Figure 3) yielded 1-1.5 orders of magnitude higher lowest *K_D* estimates for Sema and Lira (Table 2), which may be due to differences in the buffer conditions or analyte concentrations used in the BLI and SPR experiments. For Exen, , the quality of the SPR data (Figures 3C, 3F) was insufficient for a reliable kinetic analysis, but it can be concluded that the corresponding *K_D* values reach the analyte concentration level of 1 μM. The latter estimate is slightly lower than that derived from the BLI experiments, which can be rationalized by the same factors.

The *K_D* estimates for Aβ-Sema/Lira complexes (Tables 1, 2) are comparable to those for Aβ binding to its natural depot, human serum albumin (HSA) (~0.1 μM [58]), as well as for Aβ complexes with fragments of the receptor for advanced glycation end products, which exhibit neuroprotective activity in both in vitro and in vivo models [59]. Similarly, the *K_D* values for Aβ-Sema/Lira complexes are close to the *K_D* estimate for binding of ¹²⁵I-labelled Lira to GLP-1 receptor, 1.3×10⁻⁷ M [60]. Moreover, these values are close to the peak plasma concentrations of Sema/Lira (20-120 nM [61,62]), indicating that Sema/Lira interaction with Aβ (0.5 nM in plasma [63]) may occur in the circulation.

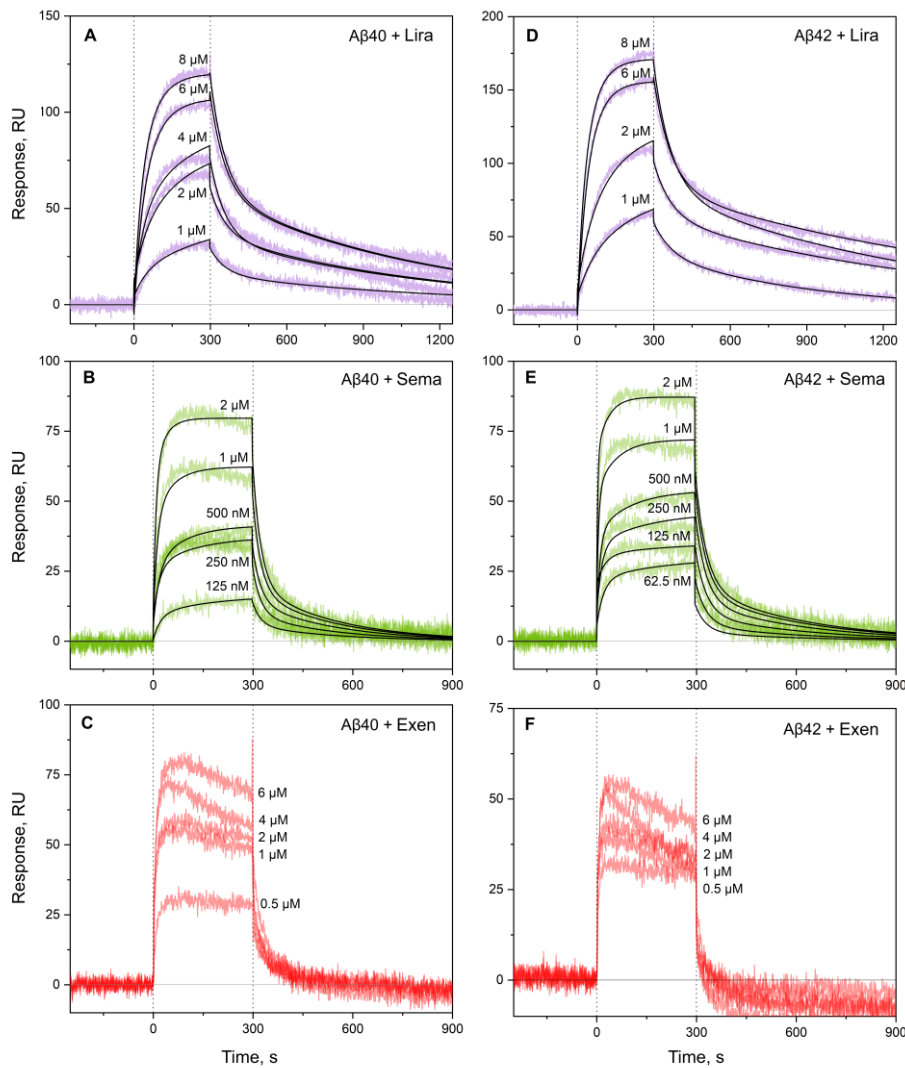


Figure 3. Kinetics of interaction between monomeric Aβ40 (panels A-C) or Aβ42 (D-F) and Lira (violet), Sema (green) or Exen (red) at 25°C, monitored using SPR (10 mM HEPES-NaOH, 150 mM NaCl, 0.05% Tween 20, pH 7.4). The analyte concentrations are indicated nearby the sensograms. The black curves are theoretical, calculated according to the heterogeneous ligand model (2) (see Table 2 for the fitting parameters).

Table 2. Parameters of the interaction between monomeric Aβ40/Aβ42 and the GLP-1RAs at 25°C, estimated from the SPR data shown in Figure 3 using the heterogeneous ligand model (2).

$[GLP-1RA], \mu M$		$k_{a1}, M^{-1}s^{-1}$	k_{d1}, s^{-1}	K_{D1}, M	$k_{a2}, M^{-1}s^{-1}$	k_{d2}, s^{-1}	K_{D2}, M
<i>Aβ40</i>							
<i>Sema</i>	0.06-2	$(9.6 \pm 2.4) \times 10^3$	$(3.2 \pm 0.9) \times 10^{-3}$	$(3.4 \pm 0.5) \times 10^{-7}$	$(3.90 \pm 1.12) \times 10^4$	$(4.32 \pm 0.12) \times 10^{-2}$	$(1.2 \pm 0.4) \times 10^{-6}$
<i>Lira</i>	1-8	$(1.44 \pm 0.05) \times 10^3$	$(1.19 \pm 0.13) \times 10^{-3}$	$(9.5 \pm 0.7) \times 10^{-7}$	$(1.9 \pm 0.3) \times 10^3$	$(1.70 \pm 0.10) \times 10^{-2}$	$(9.1 \pm 1.6) \times 10^{-6}$
<i>Aβ42</i>							
<i>Sema</i>	0.06-2	$(1.26 \pm 0.11) \times 10^4$	$(4.1 \pm 1.4) \times 10^{-3}$	$(3.4 \pm 1.4) \times 10^{-7}$	$(1.34 \pm 0.18) \times 10^5$	$(3.8 \pm 0.7) \times 10^{-2}$	$(3.0 \pm 0.9) \times 10^{-7}$
<i>Lira</i>	1-8	$(2.24 \pm 0.18) \times 10^3$	$(1.14 \pm 0.10) \times 10^{-3}$	$(5.2 \pm 0.8) \times 10^{-7}$	$(2.9 \pm 0.04) \times 10^3$	$(1.64 \pm 0.14) \times 10^{-2}$	$(5.6 \pm 0.3) \times 10^{-6}$

2.2. Concentration-Dependent Changes in Quaternary Structure of the GLP-1RAs

Since GLP-1RAs are prone to oligomerization and fibrillation [64–66], we studied the quaternary structure of GLP-1 and its analogues using dynamic light scattering (DLS) spectroscopy in a buffer with salt conditions close to physiological ones and similar to the BLI experiments (Table 3). Decrease in DLS sensitivity at protein concentrations of 0.05–0.02 mg/mL prevented the measurements at the GLP-1RAs concentrations below 6–12 μ M, depending on the peptide.

The main light scattering peak of 5-83 μ M GLP-1(7-37) corresponds to particles with a hydrodynamic radius (R_h) exceeding 92 nm, which indicates strong oligomerization of the peptide and explains the inability to describe analytically the BLI data on its interaction with A β 40/A β 42 (Figures 1A, 1E).

The DLS data for 6-105 μ M Lira show an increase in its degree of multimerization, MW_{Rh}/MW_m , with protein concentration from 6.5–8.2 to 15.6, consistent with the other reports [66–68]. This transition in oligomeric state of Lira correlates with a tendency to changes in the K_D values for its interaction with A β 40/A β 42 (Table 1).

Similarly to Lira, Exen demonstrates an increase in degree of multimerization with protein concentration (15-234 μ M) from 1.6 to 5.9, in agreement with the literature data [69].

The R_h estimates for Sema (12 μ M, 47 μ M) are consistent with its monomer and dimer, which is below the previous estimates for the formulation buffer composition [66]. Hence, the K_D values for Sema interaction with A β 40/A β 42 estimated using BLI (Table 1) are close to the corresponding thermodynamic constants. In contrast, in the other cases complicated by oligomerization of the GLP-1RAs, the estimates shown in Table 1 represent only apparent constants.

Table 3. Concentration dependence of hydrodynamic radius (R_h), molecular mass (MW_{Rh}) and degree of multimerization (MW_{Rh}/MW_m) for the GLP-1RAs at 25°C, determined by DLS (25 mM Tris-HCl, 140 mM NaCl, 4.9 mM KCl, 2.5 mM CaCl₂, 1 mM MgCl₂, pH 7.4).

GLP-1RA	[GLP-1RA], μ M	R_h , nm	MW_{Rh} , kDa	MW_{Rh}/MW_m
GLP-1(7-37)	5-83	>92	>7 \times 10 ⁵	>210
Lira	105	3.08 \pm 0.15	54.7 \pm 7.8	15.6 \pm 2.2
	52	3.13 \pm 0.05	57.1 \pm 2.6	16.3 \pm 0.7
	13	2.25 \pm 0.12	22.7 \pm 6.1	6.5 \pm 1.7
	6	2.45 \pm 0.16	28.8 \pm 3.6	8.2 \pm 1.0
Exen	234	2.20 \pm 0.01	24.58 \pm 0.02	5.88 \pm 0.04
	115	2.27 \pm 0.16	26.7 \pm 5.7	6.4 \pm 1.4
	29	1.53 \pm 0.06	8.8 \pm 0.9	2.1 \pm 0.2
	15	1.39 \pm 0.07	6.7 \pm 0.9	1.6 \pm 0.2
Sema	47	1.22 \pm 0.04	4.1 \pm 0.4	1.2 \pm 0.1
	12	1.42 \pm 0.15	6.2 \pm 2.1	1.9 \pm 0.6

Overall, the DLS data indicate that the GLP-1Ras, at the concentrations used in the BLI experiments, exist as mixture of oligomers with varying degree of multimerization. However, since degree of their multimerization decreases with decreasing protein concentration, at plasma concentrations of 1-119 pM for GLP-1/Exen) [70–72] and 20-120 nM for Sema/Lira [61,62], the GLP-1RAs predominantly exist in monomeric form. In this state, hydrophobic residues and fatty acid moieties are more accessible for interaction with A β , which likely facilitates binding.

2.3. Effect of the GLP-1RAs on A β fibrillation

The influence of the GLP-1RAs on A β 40 fibril formation at 30°C was studied using ThT fluorescence assay at ThT and GLP-1RA concentrations of 10 μ M for both components (Figure 4). While Lira had no significant effect on fibrillation (Figure 4A), the other GLP-1RAs demonstrate

drastically different behavior (Figure 4B). GLP-1(7-37) and Exen both suppress A β 40 fibrillation, whereas in the presence of Sema there is a clear tendency to stimulate the fibrillation process.

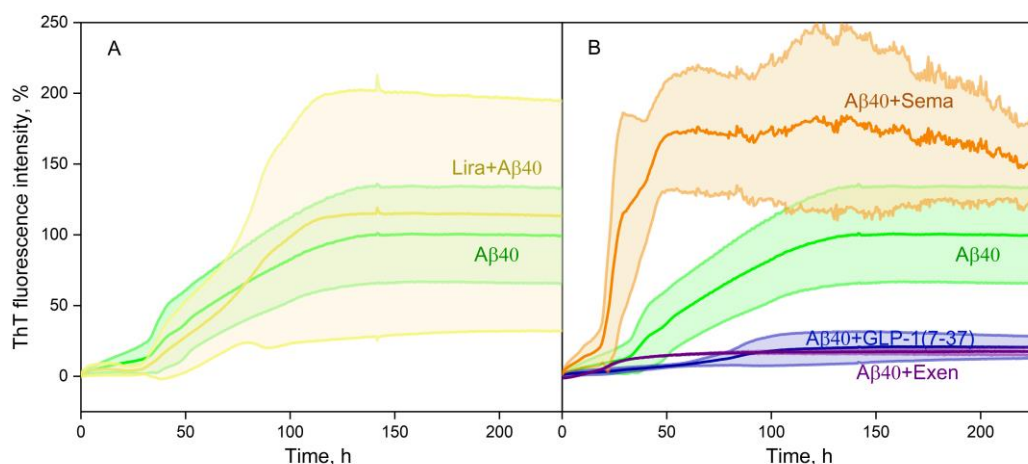


Figure 4. Kinetics of fluorescence intensity at 485 nm of 10 μ M ThT added to 20 μ M A β 40 in the absence or in the presence of 10 μ M Lira (panel A), Sema, Exen, or GLP-1(7-37) (B) at 30°C (25 mM Tris-HCl, 140 mM NaCl, 4.9 mM KCl, 2.5 mM CaCl₂, 1 mM MgCl₂, 0.05% NaN₃, pH 7.4). Standard deviations of the fluorescence signals are indicated. Excitation wavelength 440 nm.

To explore structural features of the grown fibrils, we examined them using negative-staining transmission electron microscopy, TEM (Figure 5). The A β 40 sample and samples with the addition of Lira/Sema reveal dense clusters of the intertwined mature fibrils up to 2 μ m long (Figure 5 A,B,C). When analyzing the samples with the addition of Exen, only scattered fibrils, shorter fibrils compared to the others, were visible (Figure 5D). In addition, in the presence of Exen, large clusters of fibrils, which were characteristic of the other samples, did not form (Figure 5 D). When analyzing the samples with the addition of GLP-1 sporadic small fibril clusters were still observed (Figure 5E,F). In summary, the microscopic data support the finding from the ThT fluorescence assay.

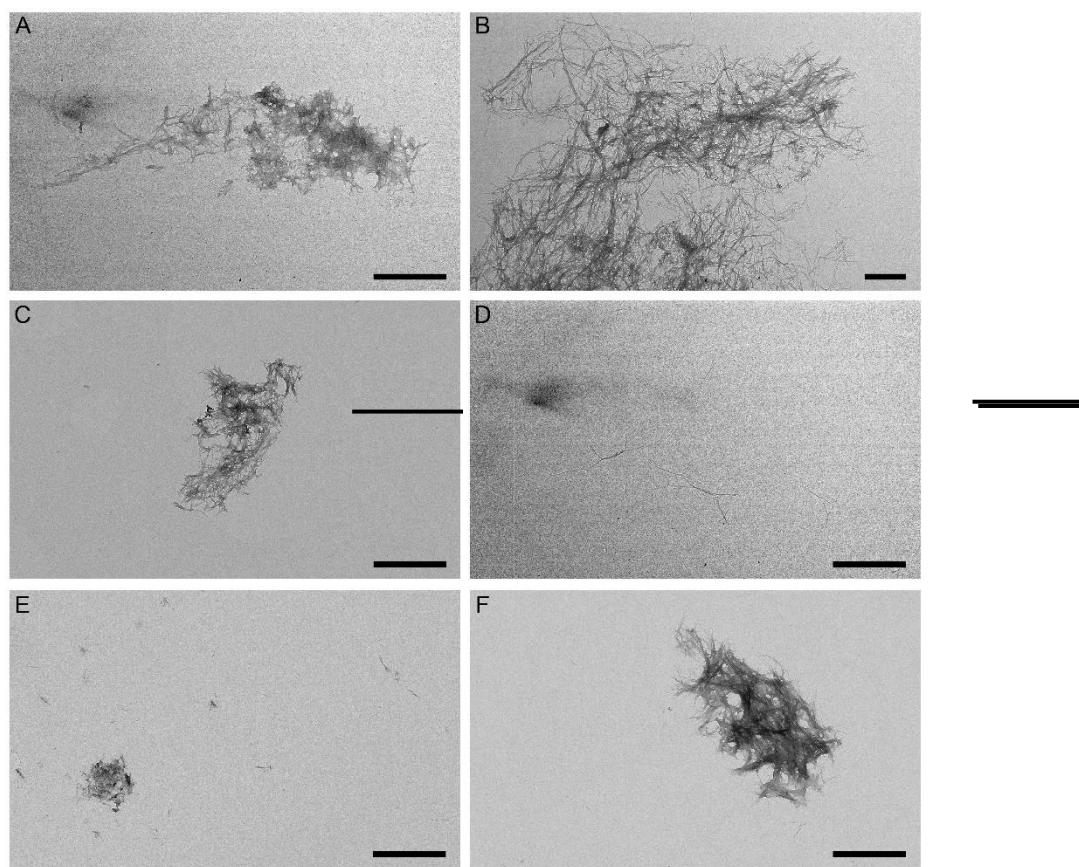


Figure 5. Negative-staining TEM images of the A β 40 fibers grown in the course of the ThT fluorescence assay shown in Figure 4 in the absence (panel **A**) or in the presence of 10 μ M Lira (**B**), 10 μ M Sema (**C**), 10 μ M Exen (**D**), GLP-1(7-37) (**E**, **F**). The scale bars represent 1 μ m .

Apparently, the ability of a particular GLP-1RA to affect A β fibrillation in vivo depends not only on its in vitro activity, but also on its ability to penetrate the CNS and distribute across the brain regions. Since Exen and GLP-1 readily cross the BBB [24,73], and GLP-1 can be expressed by some population of neurons [22,23], these GLP-1RAs have the potential to suppress A β fibrillation also in the brain tissue. On the contrary, Sema does not cross the BBB [74], indicating that its ability to stimulate A β fibrillation in vitro (Figures 4B, 5C) is unlikely to be of physiological significance.

Our in vitro data for Exen are consistent with data showing reduced A β accumulation in the AD models [40,41]. Interestingly, Lira and Sema are also able to reduce A β deposits in AD mouse models [47–49,55]. These GLP-1 analogues did not inhibit the process of fibrillation (Figures 4, 5), but in this case other mechanisms are probably involved, such as influence on APP level [47], on insulin signaling and insulin secretion level [75–77], as well as reduction of chronic inflammation level [12,49].

2.4. Structural Modeling of the Complexes Between A β 40 or Its Protofibril and GLP-1(7-37)/Exen

To identify structural patterns in the formation of the GLP-1RA–A β complexes, tertiary structures of the complexes between GLP-1(7-37)/Exen and A β 40 monomer were modeled using ClusPro docking server [78] (Figures 6A, 6B). Additionally, we investigated the interaction of GLP-1(7-37)/Exen with the protofibrillar form of A β 40, since this type of interaction (as well as interaction with monomeric A β 40) may underlie the inhibitory effects of GLP-1(7-37)/Exen on A β 40 fibril formation that we observed.

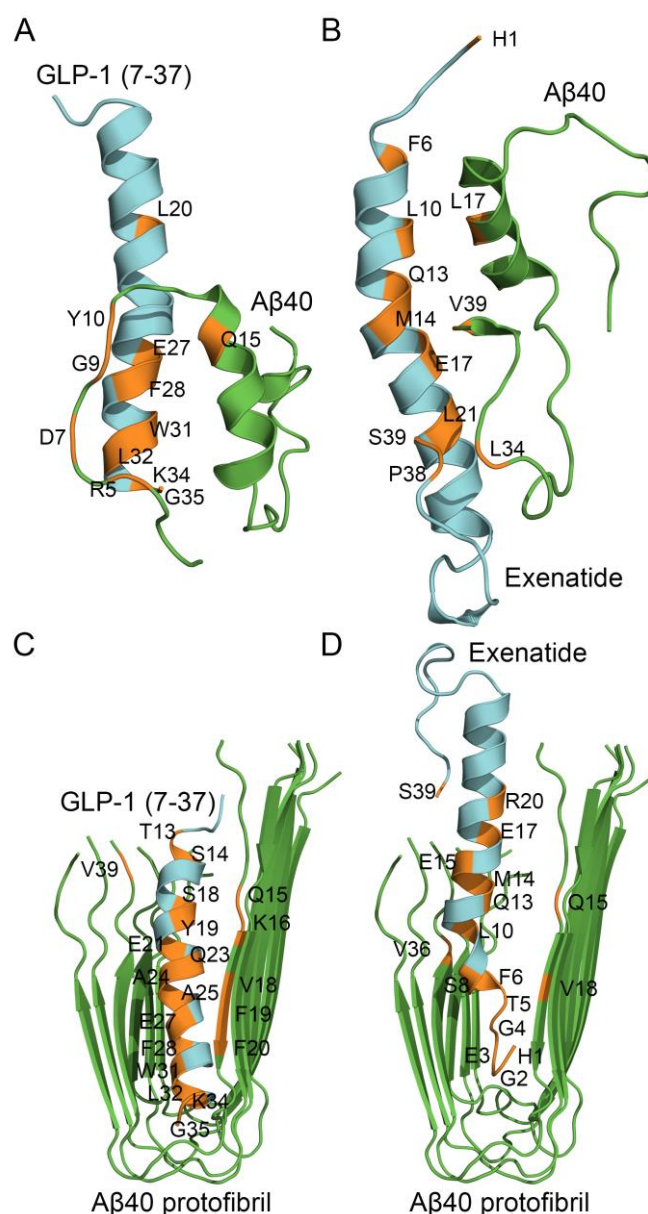


Figure 6. The models of tertiary structures of the complexes between monomeric A β 40 (taken from PDB entry 2LFM, model 1) or A β 40 protofibril (PDB entry 2LMN, model 1) (shown in green) and GLP-1(7-37) (PDB entry 3IOL, chain B) (panels A, C) or Exen (PDB entry 1JRJ, chain A) (B, D) (colored cyan) built using ClusPro docking server. The contact residues are shown in orange. The numbering of the residues is according to the PDB entries.

The modeling of the complex between GLP-1(7-37) and A β 40 monomer predicts (Figure 6A) that A β 40 binds GLP-1(7-37) via N-terminal residues R5, D7, G9, Y10, and Q15 from the α -helix. The predicted A β 40-binding site of GLP-1(7-37) includes residues L20, E27, F28, W31, L32, K34, and G35. The modeling of structure of the Exen complex with A β 40 monomer predicts (Figure 6B) that A β 40 binds Exen via residue L17 (α -helix) and C-terminal residues L34 and V39. The predicted A β 40-binding site of Exen includes N-terminal H1, residues F6, L10, Q13, M14, E17, L21 (α -helix), and C-terminal residues P38 and S39. Thus, the predicted A β 40-binding sites of GLP-1(7-37)/Exen are located in the region of residues 5-21 a.a. Meanwhile, the predicted contact residues of the A β 40 molecule differ significantly for GLP-1(7-37) and Exen, which may reflect limitations of the rigid-body approximation employed in the docking algorithm.

The modeling of the complex between GLP-1(7-37) and A β 40 protofibril predicts (Figure 6C) that GLP-1(7-37) interacts with chains A and C of the protofibril via residues T13, S14, S18, Y19, E21, Q23, A24, A25, E27, F28, W31, L32, K34, and G35. The chains A and C are predicted to bind GLP-1(7-

37) via residues Q15, K16, V18, F19, F20 and V39. Note that the same residues of GLP-1(7-37) (L20, E27, F28, W31, L32, K34, and G35) participate in the binding of both the A β 40 monomer and A β 40 protofibril.

The analogous modeling of the complex between Exen and A β 40 protofibril predicts (Figure 6D) that Exen interacts with chains A and C of the protofibril via residues H1, G2, E3, G4, T5, F6, S8, L10, Q13, M14, E15, E17, R20, and S39. The chains A and C are predicted to bind Exen via residues Q15, V18 and V36. The residues H1, F6, L10, Q13, M14, E17, are common for the binding sites of Exen with A β 40 monomer and A β 40 protofibril

The structural modeling results may explain the inhibition of A β 40 fibrillation by GLP-1(7-37)/Exen observed in vitro (Figures 4, 5), since A β 40 residues may involve in binding to GLP-1(7-37)/Exen but in the formation of mature fibrils.

2.5. Effect of the GLP-1RAs on A β Cytotoxicity to Human Neuroblastoma Cells

Since the deleterious effects of A β on neuronal cells are thought to be mediated by its oligomeric forms with increased cytotoxicity [9,79,80], we compared cytotoxicity of A β 40/A β 42 alone and in the presence of GLP-1(7-37) or its analogues against human neuroblastoma SH-SY5Y cells using the MTT assay. GLP-1RAs were premixed with A β 40/A β 42 at an equimolar ratio in the serum-free medium and added to the SH-SY5Y cells cultured in the same medium to a final concentration of the both components of 10 μ M. Staining by the MTT was performed after incubation of the cells for 48 h.

In the absence of A β , Lira, Sema and Exen have no effect on survival of SH-SY5Y cells, whereas GLP-1(7-37) enhances cell viability by 33% (Figure 7A). The addition of A β 40 or A β 42 alone decreases the cell survival by 22% and 37%, respectively (Figures 7B, 7C). The addition of Lira, Sema or Exen with A β 40/A β 42 abolishes this effect. Meanwhile, the addition of GLP-1(7-37) increases the cytotoxicity of A β 40 (Figure 7B), but does not affect the cytotoxic effect of A β 42 (Figure 7C).

The most pronounced increase in viability of SH-SY5Y cells was observed for Lira, Sema and Exen upon treatment of the cells with A β 42 (Figure 7C). Similarly, Sema reversed the effect of A β (25-35) on SH-SY5Y cells after their pretreatment with the latter [81]. Pretreatment of neuronal cells with Lira or Exen also protected them from A β (25-35) and A β 42, respectively [30,37,82].

The protective effect of Exen on the A β -treated neuroblastoma cells is consistent with results of the A β fibrillation experiments (Figures 4, 5) and rescuing memory deficits in AD mice [40]. However, such benefits have not been replicated in clinical trials [43]. Despite its higher affinity for monomeric A β , Lira exhibits a similar set of the properties, except for the lack of significant effect on A β 40 fibrillation (Table 4). In contrast, both Sema and GLP-1(7-37) show conflicting results in the A β fibrillation and A β cytotoxicity tests (Table 4), which may reflect differences in the cytotoxic properties of the multimeric forms of A β formed in their presence. In the case of Sema, the rapid fibrillation of A β 40 (Figure 4B) may prevent the accumulation of the more cytotoxic A β 40 oligomers [9,79,80]. The excess of the latter in the case of GLP-1(7-37) appears to favor its cytotoxicity, despite the suppression of A β 40 fibrillation in its presence (Table 4).

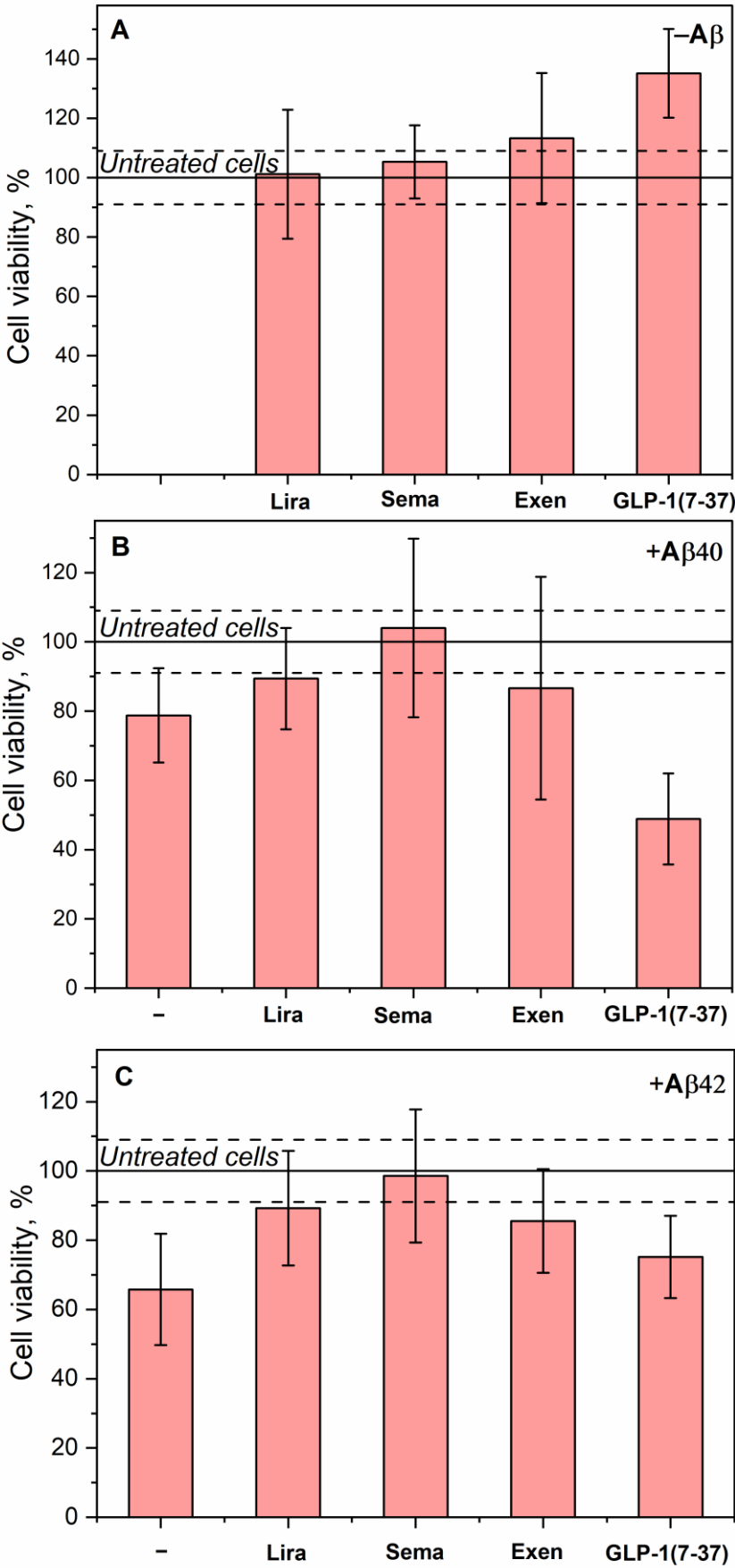


Figure 7. Effect of 10 μ M A β 40/A β 42 and/or 10 μ M Lira/Sema/Exen/GLP-1(7-37) on viability of SH-SY5Y cells assessed by an MTT assay (serum-free medium, 5% CO₂, 37°C, incubation for 48 h). **A**, effect of the GLP-1RAs on the cell viability. **B**, effect of A β 40 and the GLP-1RAs in the presence of A β 40 on the cell viability. **C**, effect of A β 42 and the GLP-1RAs in the presence of A β 42 on the cell viability. Mean values and standard deviations are indicated.

Table 4. Summary of the properties of the GLP1-RAs obtained in this work and described in the literature. The counteracting effects are highlighted in bold.

	<i>Minimal K_D for Aβ Binding According to BLI</i>	<i>Effect on Aβ40 Fibrillation (Figures 4, 5)</i>	<i>Effect on Aβ Cytotoxicity to SH-SY5Y Cells (Figure 7)</i>	<i>Ability to Cross the BBB</i>	<i>AD Animal Data</i>	<i>Clinical Data, AD</i>
Lira	4.2 \times 10 ⁻⁸ M	No effect	Protection	+ [47]	Prevents memory loss, reduces A β amyloid deposits [47–49]	No effect [50]
Sema	1.1 \times 10 ⁻⁵ M	Stimulation	Protection	– [74]	Positive effects on cognitive function, reduction of A β amyloid deposits [55]	Phase 3 clinical trials (NCT04777396 and NCT04777409)
Exen	~(0.4–1.5) \times 10 ⁻⁵ M	Inhibition	Protection	+ [73]	Positive effects on learning and memory ability, reduces A β deposition [38–41]	No effect [43]
GLP-1(7-37)	~(2.5–5.0) \times 10 ⁻⁵ M	Inhibition	Increases A β 40 cytotoxicity	+ [24]	Positive effects on learning and memory [29]	No data

3. Materials and Methods

3.1. Materials

Lira (Victoza, 6 mg/mL) and Sema (Ozempic, 1.34 mg/mL) were bought from Novo Nordisk (Bagsværd, Denmark). Exen (Byetta, 250 μ g/mL) was from Astra Zeneca (Cambridge, UK) and Acme Biochemical Technology Co., Ltd. (Shanghai, China). GLP-1(7-37) was purchased from Merck KGaA (Darmstadt, Germany), cat. #G9416, and Aladdin (Riverside, USA), cat. #G-118964. Lira, Sema and Exen were dialyzed three times against 1,000-fold excess of deionized water and then dialyzed twice against 50 mM Tris-HCl, 280 mM NaCl, 9.8 mM KCl, 5 mM CaCl₂, 2 mM MgCl₂, pH 7.4 (buffer A) for all experiments except for BLI and SPR.

Human A β 40/A β 42 was expressed in *E. coli* and purified as described earlier [83]. Briefly, chimera of A β with ubiquitin was purified using Ni-NTA affinity chromatography and cleaved with Usp2-cc protease (prepared mainly as described in ref. [84]), followed by purification using Ni-NTA and C18 columns. Quality of the A β samples was controlled by SDS-PAGE and electrospray ionization mass spectrometry.

Protein concentrations were measured spectrophotometrically using molar extinction coefficients at 280 nm calculated according to ref. [85]: 6,990 M⁻¹cm⁻¹ for Sema and Lira, 5,500 M⁻¹cm⁻¹ for Exen, and 1,490 M⁻¹cm⁻¹ for A β 40/A β 42 at pH 7.4–8.0.

Ethylenediaminetetraacetic acid (EDTA), magnesium chloride, Thioflavin T (ThT), ethanolamine and polyethylene glycol sorbitan monolaurate (TWEEN®) 20 were from Merck KGaA (Darmstadt, Germany). 2-mercaptoethanol (2-ME) was from Amresco® LLC (Vienna, Austria). Urea,

imidazole, sodium hydroxide, sodium dodecyl sulfate (SDS) and glycerol were purchased from PanReac AppliChem (Barcelona, Spain). Calcium/magnesium chloride were from Honeywell Fluka (Charlotte, NC, USA). AbiFlow 100 Ni-NTA Agarose was from Abisense (Sirius, Russia). Hydrochloric acid was from Sigma Tec LLC (Khimki, Russia). Ultra-grade Tris, HEPES, sodium chloride and dimethyl sulfoxide (DMSO) were from Helicon (Moscow, Russia). Trifluoroacetic acid (TFA) was purchased from Fisher Scientific Inc. (Waltham, USA). Potassium chloride, Coomassie Brilliant Blue R-250, 3-(4,5-dimethylthiazol-2-yl)-2,5-diphenyltetrazolium bromide (MTT) and sodium azide were from Dia-M (Moscow, Russia). Acetic acid and ammonium hydroxide were from Chimmed (Moscow, Russia) and Component-reaktiv (Moscow, Russia), respectively. Dulbecco's Modified Eagle Medium (DMEM), Fetal Bovine Serum (FBS) and penicillin-streptomycin-glutamine were from Gibco (New York, USA). Ampicillin was bought from neoFroxx (Einhausen, Germany). F12 was from PanEco (Moscow, Russia). Stock solution of ThT (0.6 mg/mL) was prepared in deionized water. ThT concentration was measured spectrophotometrically using the molar extinction coefficient at 412 nm of $36,000 \text{ M}^{-1}\text{cm}^{-1}$ [86].

Neuroblastoma SH-SY5Y cells were from Prof. Valery P. Zinchenko (Institute of Cell Biophysics of the RAS, Pushchino, Russia).

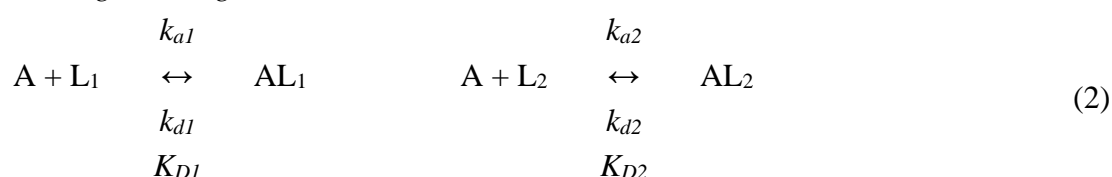
3.2. BLI Measurements

GLP-1RAs were dialyzed three times against 1,000-fold excess of deionized water and then dialyzed twice against 20 mM Tris-HCl, 140 mM NaCl, 4.9 mM KCl, 2.5 mM CaCl_2 , 1 mM MgCl_2 , pH 7.4 buffer for Exen and Lira or 20 mM HEPES-KOH, 140 mM NaCl, 4.9 mM KCl, 2.5 mM CaCl_2 , 1 mM MgCl_2 , pH 7.4 for Sema. GLP-1(7-37) was dissolved in the last buffer. The $\text{A}\beta$ samples were pretreated by TFA and dissolved in DMSO (2 mg/mL) as described in ref. [58], and stored at -20°C .

Affinity of $\text{A}\beta_{40}/\text{A}\beta_{42}$ (ligand) for Exen (4–15 μM), Lira (5–20 μM), Sema (17–38 μM) or GLP-1(7-37) (25–50 μM) (analyte) at 25°C was measured by BLI using a ForteBio Octet® QKe System, 96-well microplates with shaking at 1,000 rpm. $\text{A}\beta_{40}/\text{A}\beta_{42}$ (0.05 mg/mL in 10 mM sodium acetate, pH 4.5 buffer) was immobilized on five amino-reactive biosensors while one reference sensor was loaded with 1 M ethanolamine solution through 1-ethyl-3-[3-dimethylaminopropyl]carbodiimide hydrochloride/N-hydroxysulfosuccinimide (EDAC/sulfo-NHS) reaction until the $\text{A}\beta_{40}/\text{A}\beta_{42}$ loading level of 3.5 nm was reached. The rest of the activated amine groups on the biosensors was blocked by 1 M ethanolamine solution. The non-covalently bound $\text{A}\beta_{40}/\text{A}\beta_{42}$ molecules were washed off with 0.5% SDS and then with an assay buffer (20 mM HEPES-KOH/Tris-HCl, 140 mM NaCl, 4.9 mM KCl, 2.5 mM CaCl_2 , 1 mM MgCl_2 , pH 7.4). The loading level after the washing was 1.5 nm. Baseline collection time was 300 s, association with an analyte in the assay buffer was recorded for 600 s, and dissociation phase for 600 s or 1,200 s. The ligand was regenerated by triple immersion in 0.1 % SDS water solution for 5 sec, followed by a 30 sec rinsing with the assay buffer. The BLI signal was corrected for baseline drift and non-specific binding by subtraction of the signal from the reference sensor, and fit to the *single binding site* model (A, analyte; L, ligand):



or the heterogeneous ligand scheme:



where k_a and k_d are kinetic association and dissociation constants, respectively, and K_D are equilibrium dissociation constants. The constants were evaluated for each analyte concentration using ForteBio Data Analysis software v.12.0 (Fremont, CA, USA); standard deviations are indicated.

3.3. SPR Measurements

SPR studies of Exen, Sema and Lira interaction with monomeric A β 40/A β 42 were performed at 25°C using a Bio-Rad ProteOn™ XPR36 instrument mainly according to ref. [87]. Lira and Sema were exhaustively dialyzed against 10 mM sodium phosphate, 50 mM NaCl, pH 7.0 buffer. Exen was exhaustively dialyzed against buffer A. Concentrations of stock solutions were 70–243 μ M for Sema, 1,4–2,0 mM for Lira and 27 μ M for Exen. The A β samples were pretreated by TFA and dissolved in DMSO (2 mg/mL) as described in ref. [58], and stored at –20°C.

Ligand (50 μ g/mL A β 40/A β 42) was immobilized on a ProteOn GLH sensor chip surface by amine coupling using EDAC/sulfo-NHS, with subsequent blocking of the remaining activated amine groups on the chip surface by 1 M ethanolamine solution. The noncovalently bound A β 40/A β 42 molecules were washed off the chip surface with a 0.5% SDS water solution. Analyte (0.0625–2 μ M Sema, 1–8 μ M Lira and 0.5–6 μ M Exen) in the running buffer (10 mM HEPES-NaOH, 150 mM NaCl, 0.05% Tween 20, pH 7.4) was passed over the sensor at a rate of 30 μ L/min for 300 s (association phase), followed by flushing the chip with the running buffer for 900 s (dissociation phase). The ligand was regenerated by passage of 10 mM glycine, pH 3.3 buffer, for 50 s. The kinetic SPR data were corrected for baseline drift and non-specific binding, and described using a *heterogeneous ligand* model (2). The k_a , k_d , and K_D values were estimated using Bio-Rad ProteOn Manager™ v.3.1 software (Bio-Rad Laboratories, Inc., Hercules, CA, USA). The estimates were performed for each data set globally, followed by their averaging; standard deviations are indicated.

3.4. Dynamic Light Scattering Measurements

DLS measurements were carried out using a Zetasizer Nano ZS system (Malvern Instruments Ltd., Malvern, UK). The backscattered light from a 4 mW He-Ne laser 632.8 nm was collected at an angle of 173°. Lira (6–105 μ M), Exen (15–234 μ M), Sema (12–47 μ M) and GLP-1(7–37) (5–83 μ M) solutions in 25 mM Tris-HCl, 140 mM NaCl, 4.9 mM KCl, 2.5 mM CaCl₂, 1 mM MgCl₂, pH 7.4 buffer were incubated at 25°C for 3 min. The acquisition time for a single autocorrelation function was 100 s. The resulting autocorrelation functions are averaged values from three measurements. The volume-weighted size distributions were calculated using the following parameters for the buffer: refractive index of 1.334 measured with RL3 refractometer (PZO, Warszawa, Poland); the viscosity value η = 0.95 mPa·s measured using micro-rheology method with a water suspension of standard latex nanoparticles (NIST 3060A, Thermo Fisher Scientific, USA). Molecular mass and its standard deviation corresponding to the volume-weighted hydrodynamic radius MW_{Rh} distribution was calculated in approximation of a globular protein according to the equations from ref. [88]. Degree of multimerization was calculated as a MW_{Rh}/MW_m ratio, where MW_m is a molecular mass of monomeric GLP-1RAs calculated from its molecular structure.

3.5. Structural Modeling

The unrelaxed structure of Sema was built in PyMOL v.2.0 software (Schrödinger, Inc., New York, USA) based on the structure of Sema- and taspeglutide-bound GLP-1 receptor in complex with Gs protein (PDB ID: 7KI0, EM, chain E) by combination with a linker and C18 di-acid chain (Figure 1B). Structures of the linker and C18 di-acid chain were built using ChemDraw v.22 (Boston, USA) and minimized in the MM2 field (ChemDraw v.22).

The tertiary structures of A β 40 (PDB ID 2LFM, NMR, model 1), A β 40 fibril (PDB ID 2LMN, NMR, model 1), Exen (PDB ID 1JRJ, NMR, chain A, model 1) and GLP-1(7–37) (PDB ID 3IOL, X-ray, chain B) were taken from PDB (www.rcsb.org [89]). Models of tertiary structures of A β 40/protofibril complexes with Exen or GLP-1(7–37) were built using ClusPro docking server [78]. The resulting

complexes were visualized and analyzed using PyMOL v.2 (<https://pymol.org>). The contact residues in the docking models were calculated using a PyMOL script. The numbering of the contact residues is according to the PDB entries.

3.6. ThT Fluorescence Assay

ThT fluorescence emission measurements were carried out mainly as described in ref. [83] using a BioTek Synergy H1 microplate reader, emission wavelength of 485 nm and excitation at 440 nm. A β 40 sample was prepared as described in the ref. [83] with some modifications (~ 5 mM NaOH at pH 11.8, 0.5 mg/mL). 20 μ M A β 40 was incubated at 30°C in the absence/presence of 10 μ M Sema, Lira, Exen or GLP-1(7-37). The control curves (without A β 40; Figure S1) were subtracted from the corresponding kinetic curves of A β 40 samples with/without GLP-1RAs. Each measurement was performed in 2-10 repetitions. The mean fluorescence signal values for each experimental sample were normalized to the average fluorescence signal corresponding to the saturation phase of A β 40 fibril formation without additives. Data are presented as mean \pm standard deviation.

3.7. Transmission Electron Microscopy

A copper grid (300-mesh) coated with a 0.2% formvar film was placed on a 10 μ L drop of the sample. After incubating the sample (following the ThT fluorescence assay) for 15 minutes to allow adsorption, the grid was stained with a 1% (w/v) aqueous solution of uranyl acetate for 2 minutes. Excess stain was removed using filter paper, and the grid was rinsed in deionized water for 1 minute. The samples were analyzed using a JEM-1400Plus (HC) transmission electron microscope (JEOL, Ltd., Tokyo, Japan) at an accelerating voltage of 80 keV.

3.8. Cell Viability Assay

Human neuroblastoma SH-SY5Y cells were cultured in DMEM-F12 medium supplemented with 1% penicillin-streptomycin-glutamine and 10% fetal bovine serum at 37°C for 24 h in a humidified atmosphere with 5% CO₂. Upon reaching 80% confluence, the cells were harvested and seeded into 96-well plates at a density of 15×10^5 cells per well in the serum-free DMEM/F12+PSG medium.

The A β 40/A β 42 samples were dissolved in fresh 1% NH₄OH at a concentration of 0.5 mg/mL, followed by freeze-drying. The dried A β 40/A β 42 samples were dissolved in serum-free DMEM medium at a concentration of 40-50 μ M (0.17-0.23 mg/mL), followed by mixing with the GLP-1RA (Sema, Lira, Exen or GLP-1) stock solutions in buffer A and the same medium to a final concentration of the both components of 20 μ M.

Freshly prepared A β 40/A β 42, GLP-1RAs, or their mixtures were added (100 μ L per well) to the cultures 24 h after seeding to a final concentration of the both components of 10 μ M. The final volume of medium in the well was 200 μ L. The MTT assay, designed to assess cellular metabolic activity, was performed after incubation of the cells for 48 h. 0.005 mg/mL MTT was added and the cells were incubated for 3 h, followed by solubilization of the cells using DMSO. Absorbance at 550 nm was measured using an BioTek Synergy H1 microplate reader (Agilent Technologies, Inc., Santa Clara, CA, USA). The resulting values were normalized relative to the control group of the untreated cells (100%). Data are presented as mean \pm standard deviation (n=5-10).

4. Conclusions

The risk of AD development in patients with diabetes increases by approximately 65% [8], since these diseases share some pathological features [12]. Therefore, antidiabetic drugs, including GLP-1RAs, are now being repurposed for treatment of AD [14]. Although both animal studies and clinical trials have reported beneficial effects of GLP-1RAs on the course of AD [29,36,85], the molecular mechanisms underlying these effects remain poorly understood. Here we demonstrated direct interaction of GLP-1RAs such as GLP-1(7-37), Lira, Sema and Exen with monomeric forms of A β 40 and A β 42 under the in vitro conditions mimicking physiological conditions. Comparison of the K_D

estimates for A β -Sema/Lira complexes with peak plasma concentrations of Sema/Lira indicates potential physiological significance of these interactions. This suggestion is supported by the marked effect of Sema on A β 40 fibrillation in vitro and the effect of Sema/Lyra on A β -induced cytotoxicity towards SH-SY5Y cells. Similarly, Exen and GLP-1(7-37) affect A β 40 fibrillation and cytotoxicity of A β against SH-SY5Y cells. Notably, these effects largely depend on the specific GLP-1RA and not necessarily correlate with results of animal and clinical studies (Table 4). The latter also depends on the ability of GLP-1RA to cross the BBB, which is only possessed by Exen, Lira and GLP-1(7-37), but not by Sema.

Our findings indicate that, despite certain structural similarities, individual GLP-1RAs exhibit distinct behaviors in vitro in terms of their affinity for A β , their influence on A β fibril formation, and their modulation of A β -associated cytotoxicity (Table 4). Further clinical trials of GLP-1-based drugs are needed to rule out the possibility of neuronal damage that does not necessarily lead to progression of AD. Our findings not only suggest a new mechanism for the influence of GLP-1RAs on A β metabolism in vivo, but also provide a basis for the development of GLP-1RA drugs with more pronounced anti-AD effects.

Supplementary Materials: The following supporting information can be downloaded at the website of this paper posted on Preprints.org, Figure S1: The change in ThT fluorescence in solutions with and without Sema (10 μ M), Lira (10 μ M), GLP-1 (10 μ M), Exen (10 μ M) over time. Buffer: 25 mM Tris-HCl, 140 mM NaCl, 4.9 mM KCl, 2.5 mM CaCl₂, 1 mM MgCl₂, 0.05% NaN₃, pH 7.4.

Author Contributions: Conceptualization, E.L., M.Sh., E.N.; methodology, E.D., E.L., M.Sh., A.Ch., V.R.; software, E.D., A.M., V.D.; validation, E.L., M.Sh., E.D., A.Ch., A.V.; formal analysis, M.Sh., E.D., E.L., E.N.; investigation, E.L., M.Sh., V.R., A.V., A.M., E.D., V.A., A. Ch.; resources, M.P., V.A., A.N.; data curation, E.L., M.Sh., V.R., S.P.; writing—original draft preparation, E.L., E.D., M.Sh., A.Ch., V.R.; writing—review and editing, S.P., E.N.; visualization, E.L., M.Sh., E.D., V.R., A.Ch., A.M.; supervision, E.L., E.N.; project administration, E.L.; funding acquisition, E.L. All authors have read and agreed to the published version of the manuscript.

Funding: This research was funded by Russian Science Foundation, grant number 20-74-10072, <https://rscf.ru/project/20-74-10072/>. The funders had no role in study design, data collection and analysis, decision to publish, or preparation of the manuscript.

Institutional Review Board Statement: Not applicable.

Informed Consent Statement: Not applicable.

Data Availability Statement: Data are contained within the article and supplementary materials.

Acknowledgments: We are grateful to Dr. Roman Fadeev (ITEB RAS, Pushchino, Russia) for preliminary data on influence of the GLP-1RAs on A β cytotoxicity. The authors are grateful to Vadim V. Rogachevskii (Institute of Cell Biophysics, Russian Academy of Sciences, Pushchino, Moscow Region, Russia) for providing access to the electron microscope of the Shared Core Facilities of the Pushchino Scientific Center for Biological Research (<http://www.ckp-rf.ru/ckp/670266/>; accessed on 25 March 2025).

Conflicts of Interest: The authors declare no conflicts of interest.

Abbreviations

2-ME	2-mercaptoethanol
A β	amyloid- β peptide
A β 40/A β 42	amyloid- β peptide, residues 1-40/42
AD	Alzheimer's disease
APP	amyloid precursor protein
BBB	blood-brain barrier
CNS	central nervous system
DM	diabetes mellitus

DM2	type 2 diabetes mellitus
DMEM	Dulbecco's Modified Eagle Medium
DMSO	dimethyl sulfoxide
DPP-4	dipeptidyl peptidase-4
EDAC/sulfo-NHS	1-ethyl-3-[3-dimethylaminopropyl]carbodiimide hydrochloride/N-hydroxysulfosuccinimide
EDTA	ethylenediaminetetraacetic acid
EM	Electron microscope
Exen	Exendin-4/Exenatide
GLP-1	glucagon-like peptide 1
GLP-1(7-36), GLP-1(7-37)	N-terminally truncated forms of glucagon-like peptide 1, residues 7-36 or 7-37
GLP-1R	glucagon-like peptide 1 receptor
GLP-1RA	glucagon-like peptide 1 receptor agonist
HSA	human serum albumin
Lira	Liraglutide
MTT	3-(4,5-dimethylthiazol-2-yl)-2,5-diphenyltetrazolium bromide
MW _m	molecular mass calculated from the amino acid sequence
MW _{Rh}	molecular mass calculated from the hydrodynamic radius
NMR	nuclear magnetic resonance
PA	palmitic acid
PDB	Protein Data Bank
Sema	Semaglutide
SDS	sodium dodecyl sulfate
TEM	transmission electron microscopy
TFA	trifluoroacetic acid
ThT	Thioflavin T
Tris	tris(hydroxymethyl)aminomethane
TWEEN	polyethylene glycol sorbitan monolaurate

References

1. Gustavsson, A.; Norton, N.; Fast, T.; Frölich, L.; Georges, J.; Holzapfel, D.; Kirabali, T.; Krolak-Salmon, P.; Rossini, P.M.; Ferretti, M.T.; et al. Global estimates on the number of persons across the Alzheimer's disease continuum. *Alzheimer's & dementia : the journal of the Alzheimer's Association* **2023**, *19*, 658-670, doi:10.1002/alz.12694.

2. Harris, E. FDA Green-Lights Second Alzheimer Drug, Donanemab. *JAMA* **2024**, *332*, 524-524, doi:10.1001/jama.2024.13386.

3. 2024 Alzheimer's disease facts and figures. *Alzheimer's & Dementia* **2024**, *20*, 3708-3821, doi:https://doi.org/10.1002/alz.13809.

4. Ameen, T.B.; Kashif, S.N.; Abbas, S.M.I.; Babar, K.; Ali, S.M.S.; Raheem, A. Unraveling Alzheimer's: the promise of aducanumab, lecanemab, and donanemab. *The Egyptian Journal of Neurology, Psychiatry and Neurosurgery* **2024**, *60*, 72, doi:10.1186/s41983-024-00845-5.

5. Sadigh-Eteghad, S.; Sabermarouf, B.; Majdi, A.; Talebi, M.; Farhoudi, M.; Mahmoudi, J. Amyloid-beta: a crucial factor in Alzheimer's disease. *Med Princ Pract* **2015**, *24*, 1-10, doi:10.1159/000369101.

6. O'Brien, R.J.; Wong, P.C. Amyloid precursor protein processing and Alzheimer's disease. *Annu Rev Neurosci* **2011**, *34*, 185-204, doi:10.1146/annurev-neuro-061010-113613.

7. Glenner, G.G.; Wong, C.W. Alzheimer's disease: initial report of the purification and characterization of a novel cerebrovascular amyloid protein. *Biochem Biophys Res Commun* **1984**, *120*, 885-890, doi:S0006-291X(84)80190-4 [pii]10.1016/s0006-291x(84)80190-4.

8. Chen, G.F.; Xu, T.H.; Yan, Y.; Zhou, Y.R.; Jiang, Y.; Melcher, K.; Xu, H.E. Amyloid beta: structure, biology and structure-based therapeutic development. *Acta Pharmacol Sin* **2017**, *38*, 1205-1235, doi:aps201728 [pii]10.1038/aps.2017.28.

9. Vander Zanden, C.M.; Wampler, L.; Bowers, I.; Watkins, E.B.; Majewski, J.; Chi, E.Y. Fibrillar and Nonfibrillar Amyloid Beta Structures Drive Two Modes of Membrane-Mediated Toxicity. *Langmuir* **2019**, *35*, 16024-16036, doi:10.1021/acs.langmuir.9b02484.
10. Arvanitakis, Z.; Wilson, R.S.; Bienias, J.L.; Evans, D.A.; Bennett, D.A. Diabetes mellitus and risk of Alzheimer disease and decline in cognitive function. *Archives of neurology* **2004**, *61*, 661-666, doi:10.1001/archneur.61.5.661.
11. Ott, A.; Stolk, R.P.; Hofman, A.; van Harskamp, F.; Grobbee, D.E.; Breteler, M.M. Association of diabetes mellitus and dementia: the Rotterdam Study. *Diabetologia* **1996**, *39*, 1392-1397, doi:10.1007/s001250050588.
12. Wang, Z.J.; Han, W.N.; Chai, S.F.; Li, Y.; Fu, C.J.; Wang, C.F.; Cai, H.Y.; Li, X.Y.; Wang, X.; Hölscher, C.; et al. Semaglutide promotes the transition of microglia from M1 to M2 type to reduce brain inflammation in APP/PS1/tau mice. *Neuroscience* **2024**, *563*, 222-234, doi:10.1016/j.neuroscience.2024.11.022.
13. Overview: Type 2 diabetes. In *InformedHealth.org [Internet]*. ; Institute for Quality and Efficiency in Health Care (IQWiG): Cologne, Germany, 2006.
14. Michailidis, M.; Moraitou, D.; Tata, D.A.; Kalinderi, K.; Papamitsou, T.; Papaliagkas, V. Alzheimer's Disease as Type 3 Diabetes: Common Pathophysiological Mechanisms between Alzheimer's Disease and Type 2 Diabetes. *Int J Mol Sci* **2022**, *23*, doi:ijms23052687 [pii]ijms-23-02687 [pii]10.3390/ijms23052687.
15. Kandimalla, R.; Thirumala, V.; Reddy, P.H. Is Alzheimer's disease a Type 3 Diabetes? A critical appraisal. *Biochim Biophys Acta Mol Basis Dis* **2017**, *1863*, 1078-1089, doi:S0925-4439(16)30215-0 [pii]10.1016/j.bbadis.2016.08.018.
16. Michailidis M; Tata DA; Moraitou D; Kavvadas D; Karachrysafi S; Papamitsou T; Vareltsis P; V., P. Antidiabetic Drugs in the Treatment of Alzheimer's Disease. *Int J Mol Sci* **2022**, *23*.
17. Mudaliar, S.; Henry, R.R. The incretin hormones: from scientific discovery to practical therapeutics. *Diabetologia* **2012**, *55*, 1865-1868, doi:10.1007/s00125-012-2561-x.
18. Cobble, M. Differentiating among incretin-based therapies in the management of patients with type 2 diabetes mellitus. *Diabetology & Metabolic Syndrome* **2012**, *4*, 8, doi:10.1186/1758-5996-4-8.
19. Meier, J. *The role of incretin-based therapies in the management of type 2 diabetes mellitus: perspectives on the past, present and future*; 2019; Volume 22.
20. Lim, G.E.; Brubaker, P.L. Glucagon-Like Peptide 1 Secretion by the L-Cell: The View From Within. *Diabetes* **2006**, *55*, S70-S77, doi:10.2337/db06-S020.
21. Drucker, D.J. Mechanisms of Action and Therapeutic Application of Glucagon-like Peptide-1. *Cell Metab* **2018**, *27*, 740-756, doi:S1550-4131(18)30179-7 [pii]10.1016/j.cmet.2018.03.001.
22. Müller, T.D.; Finan, B.; Bloom, S.R.; D'Alessio, D.; Drucker, D.J.; Flatt, P.R.; Fritsche, A.; Gribble, F.; Grill, H.J.; Habener, J.F.; et al. Glucagon-like peptide 1 (GLP-1). *Molecular metabolism* **2019**, *30*, 72-130, doi:10.1016/j.molmet.2019.09.010.
23. Holt, M.K.; Richards, J.E.; Cook, D.R.; Brierley, D.I.; Williams, D.L.; Reimann, F.; Gribble, F.M.; Trapp, S. Preproglucagon Neurons in the Nucleus of the Solitary Tract Are the Main Source of Brain GLP-1, Mediate Stress-Induced Hypophagia, and Limit Unusually Large Intakes of Food. *Diabetes* **2019**, *68*, 21-33, doi:10.2337/db18-0729.
24. Kastin, A.J.; Akerstrom, V.; Pan, W. Interactions of glucagon-like peptide-1 (GLP-1) with the blood-brain barrier. *J Mol Neurosci* **2002**, *18*, 7-14, doi:JM18:1-2:07 [pii]10.1385/JMN:18:1-2:07.
25. Muscogiuri, G.; DeFronzo, R.A.; Gastaldelli, A.; Holst, J.J. Glucagon-like Peptide-1 and the Central/Peripheral Nervous System: Crosstalk in Diabetes. *Trends Endocrinol Metab* **2017**, *28*, 88-103, doi:S1043-2760(16)30126-6 [pii]10.1016/j.tem.2016.10.001.
26. Monney, M.; Jornayvaz, F.R.; Gariani, K. GLP-1 receptor agonists effect on cognitive function in patients with and without type 2 diabetes. *Diabetes Metab* **2023**, *49*, 101470, doi:S1262-3636(23)00052-6 [pii]10.1016/j.diabet.2023.101470.
27. Holscher, C. Novel dual GLP-1/GIP receptor agonists show neuroprotective effects in Alzheimer's and Parkinson's disease models. *Neuropharmacology* **2018**, *136*, 251-259, doi:S0028-3908(18)30040-6 [pii]10.1016/j.neuropharm.2018.01.040.

28. Abbas, T.; Faivre, E.; Holscher, C. Impairment of synaptic plasticity and memory formation in GLP-1 receptor KO mice: Interaction between type 2 diabetes and Alzheimer's disease. *Behav Brain Res* **2009**, *205*, 265-271, doi:S0166-4328(09)00397-0 [pii]10.1016/j.bbr.2009.06.035.
29. During, M.J.; Cao, L.; Zuzga, D.S.; Francis, J.S.; Fitzsimons, H.L.; Jiao, X.; Bland, R.J.; Klugmann, M.; Banks, W.A.; Drucker, D.J.; et al. Glucagon-like peptide-1 receptor is involved in learning and neuroprotection. *Nat Med* **2003**, *9*, 1173-1179, doi:nm919 [pii]10.1038/nm919.
30. Perry, T.; Lahiri, D.K.; Sambamurti, K.; Chen, D.; Mattson, M.P.; Egan, J.M.; Greig, N.H. Glucagon-like peptide-1 decreases endogenous amyloid-beta peptide (A β) levels and protects hippocampal neurons from death induced by A β and iron. *Journal of neuroscience research* **2003**, *72*, 603-612, doi:10.1002/jnr.10611.
31. Qin, Z.; Sun, Z.; Huang, J.; Hu, Y.; Wu, Z.; Mei, B. Mutated recombinant human glucagon-like peptide-1 protects SH-SY5Y cells from apoptosis induced by amyloid-beta peptide (1-42). *Neurosci Lett* **2008**, *444*, 217-221, doi:S0304-3940(08)01164-6 [pii]10.1016/j.neulet.2008.08.047.
32. Ussher, J.R.; Drucker, D.J. Cardiovascular biology of the incretin system. *Endocr Rev* **2012**, *33*, 187-215, doi:er.2011-1052 [pii]10.1210/er.2011-1052.
33. Hui, H.; Farilla, L.; Merkel, P.; Perfetti, R. The short half-life of glucagon-like peptide-1 in plasma does not reflect its long-lasting beneficial effects. *European journal of endocrinology* **2002**, *146*, 863-869, doi:10.1530/eje.0.1460863.
34. Plamboeck, A.; Holst, J.J.; Carr, R.D.; Deacon, C.F. Neutral Endopeptidase 24.11 and Dipeptidyl Peptidase IV are Both Involved in Regulating the Metabolic Stability of Glucagon-like Peptide-1 in vivo. In *Dipeptidyl Aminopeptidases in Health and Disease*, Back, N., Cohen, I.R., Kritchevsky, D., Lajtha, A., Paoletti, R., Eds.; Springer US: Boston, MA, 2003; pp. 303-312.
35. Collins L, C.R. Glucagon-Like Peptide-1 Receptor Agonists. In *StatPearls [Internet]*; 2025.
36. Gupta, V. Glucagon-like peptide-1 analogues: An overview. *Indian J Endocrinol Metab* **2013**, *17*, 413-421, doi:IJEM-17-413 [pii]10.4103/2230-8210.111625.
37. Li, Y.; Duffy, K.B.; Ottinger, M.A.; Ray, B.; Bailey, J.A.; Holloway, H.W.; Tweedie, D.; Perry, T.; Mattson, M.P.; Kapogiannis, D.; et al. GLP-1 receptor stimulation reduces amyloid-beta peptide accumulation and cytotoxicity in cellular and animal models of Alzheimer's disease. *Journal of Alzheimer's disease : JAD* **2010**, *19*, 1205-1219, doi:10.3233/jad-2010-1314.
38. Wang, X.; Wang, L.; Jiang, R.; Xu, Y.; Zhao, X.; Li, Y. Exendin-4 antagonizes A β 1-42-induced attenuation of spatial learning and memory ability. *Exp Ther Med* **2016**, *12*, 2885-2892, doi:10.3892/etm.2016.3742.
39. Garabadu, D.; Verma, J. Exendin-4 attenuates brain mitochondrial toxicity through PI3K/Akt-dependent pathway in amyloid beta (1-42)-induced cognitive deficit rats. *Neurochemistry International* **2019**, *128*, 39-49, doi:https://doi.org/10.1016/j.neuint.2019.04.006.
40. Wang, Y.; Chen, S.; Xu, Z.; Chen, S.; Yao, W.; Gao, X. GLP-1 receptor agonists downregulate aberrant G α T-III expression in Alzheimer's disease models through the Akt/GSK-3 β / β -catenin signaling. *Neuropharmacology* **2018**, *131*, 190-199, doi:https://doi.org/10.1016/j.neuropharm.2017.11.048.
41. Song, X.; Sun, Y.; Wang, Z.; Su, Y.; Wang, Y.; Wang, X. Exendin-4 alleviates β -Amyloid peptide toxicity via DAF-16 in a *Caenorhabditis elegans* model of Alzheimer's disease. *Frontiers in Aging Neuroscience* **2022**, *14*, doi:10.3389/fnagi.2022.955113.
42. Aviles-Olmos, I.; Dickson, J.; Kefalopoulou, Z.; Djamshidian, A.; Kahan, J.; Ell, P.; Whitton, P.; Wyse, R.; Isaacs, T.; Lees, A.; et al. Motor and cognitive advantages persist 12 months after exenatide exposure in Parkinson's disease. *J Parkinsons Dis* **2014**, *4*, 337-344, doi:H26015442R458926 [pii]10.3233/JPD-140364.
43. Mullins, R.J.; Mustapic, M.; Chia, C.W.; Carlson, O.; Gulyani, S.; Tran, J.; Li, Y.; Mattson, M.P.; Resnick, S.; Egan, J.M.; et al. A Pilot Study of Exenatide Actions in Alzheimer's Disease. *Curr Alzheimer Res* **2019**, *16*, 741-752, doi:CAR-EPUB-100792 [pii]10.2174/1567205016666190913155950.
44. Kumar, V.; Xin, X.; Ma, J.; Tan, C.; Osna, N.; Mahato, R.I. Therapeutic targets, novel drugs, and delivery systems for diabetes associated NAFLD and liver fibrosis. *Adv Drug Deliv Rev* **2021**, *176*, 113888, doi:S0169-409X(21)00280-5 [pii]10.1016/j.addr.2021.113888.
45. Meece, J. Pharmacokinetics and Pharmacodynamics of Liraglutide, a Long-Acting, Potent Glucagon-Like Peptide-1 Analog. *Pharmacotherapy* **2009**, *29*, 33S-42S, doi:10.1592/phco.29.pt2.33S.

46. Jantrapirom, S.; Nimlamool, W.; Chattipakorn, N.; Chattipakorn, S.; Temviriyankul, P.; Inthachai, W.; Govitrapong, P.; Potikanond, S. Liraglutide Suppresses Tau Hyperphosphorylation, Amyloid Beta Accumulation through Regulating Neuronal Insulin Signaling and BACE-1 Activity. *Int J Mol Sci* **2020**, *21*, doi:ijms21051725 [pii]ijms-21-01725 [pii]10.3390/ijms21051725.
47. McClean, P.L.; Parthasarathy, V.; Faivre, E.; Hölscher, C. The diabetes drug liraglutide prevents degenerative processes in a mouse model of Alzheimer's disease. *The Journal of neuroscience : the official journal of the Society for Neuroscience* **2011**, *31*, 6587-6594, doi:10.1523/jneurosci.0529-11.2011.
48. McClean, P.L.; Hölscher, C. Liraglutide can reverse memory impairment, synaptic loss and reduce plaque load in aged APP/PS1 mice, a model of Alzheimer's disease. *Neuropharmacology* **2014**, *76 Pt A*, 57-67, doi:10.1016/j.neuropharm.2013.08.005.
49. McClean, P.L.; Jalewa, J.; Hölscher, C. Prophylactic liraglutide treatment prevents amyloid plaque deposition, chronic inflammation and memory impairment in APP/PS1 mice. *Behav Brain Res* **2015**, *293*, 96-106, doi:10.1016/j.bbr.2015.07.024.
50. Gejl, M.; Gjedde, A.; Egefjord, L.; Moller, A.; Hansen, S.B.; Vang, K.; Rodell, A.; Braendgaard, H.; Gottrup, H.; Schacht, A.; et al. In Alzheimer's Disease, 6-Month Treatment with GLP-1 Analog Prevents Decline of Brain Glucose Metabolism: Randomized, Placebo-Controlled, Double-Blind Clinical Trial. *Front Aging Neurosci* **2016**, *8*, 108, doi:10.3389/fnagi.2016.00108.
51. Watson, K.T.; Wroolie, T.E.; Tong, G.; Foland-Ross, L.C.; Frangou, S.; Singh, M.; McIntyre, R.S.; Roat-Shumway, S.; Myoraku, A.; Reiss, A.L.; et al. Neural correlates of liraglutide effects in persons at risk for Alzheimer's disease. *Behav Brain Res* **2019**, *356*, 271-278, doi:S0166-4328(18)30643-0 [pii]10.1016/j.bbr.2018.08.006.
52. Lau, J.; Bloch, P.; Schaffer, L.; Pettersson, I.; Spetzler, J.; Kofoed, J.; Madsen, K.; Knudsen, L.B.; McGuire, J.; Steensgaard, D.B.; et al. Discovery of the Once-Weekly Glucagon-Like Peptide-1 (GLP-1) Analogue Semaglutide. *J Med Chem* **2015**, *58*, 7370-7380, doi:10.1021/acs.jmedchem.5b00726.
53. Chang, Y.F.; Zhang, D.; Hu, W.M.; Liu, D.X.; Li, L. Semaglutide-mediated protection against Aβ correlated with enhancement of autophagy and inhibition of apoptosis. *J Clin Neurosci* **2020**, *81*, 234-239, doi:S0967-5868(20)31533-2 [pii]10.1016/j.jocn.2020.09.054.
54. Yang, X.; Feng, P.; Zhang, X.; Li, D.; Wang, R.; Ji, C.; Li, G.; Holscher, C. The diabetes drug semaglutide reduces infarct size, inflammation, and apoptosis, and normalizes neurogenesis in a rat model of stroke. *Neuropharmacology* **2019**, *158*, 107748, doi:S0028-3908(19)30307-7 [pii]10.1016/j.neuropharm.2019.107748.
55. Zhang, Y.; Tang, C.; He, Y.; Zhang, Y.; Li, Q.; Zhang, T.; Zhao, B.; Tong, A.; Zhong, Q.; Zhong, Z. Semaglutide ameliorates Alzheimer's disease and restores oxytocin in APP/PS1 mice and human brain organoid models. *Biomedicine & pharmacotherapy = Biomedecine & pharmacotherapie* **2024**, *180*, 117540, doi:10.1016/j.biopha.2024.117540.
56. A Research Study Investigating Semaglutide in People With Early Alzheimer's Disease (EVOKE Plus). **2024**.
57. Cummings, J.L.; Atri, A.; Feldman, H.H.; Hansson, O.; Sano, M.; Knop, F.K.; Johannsen, P.; León, T.; Scheltens, P. evoke and evoke+: design of two large-scale, double-blind, placebo-controlled, phase 3 studies evaluating efficacy, safety, and tolerability of semaglutide in early-stage symptomatic Alzheimer's disease. *Alzheimer's research & therapy* **2025**, *17*, 14, doi:10.1186/s13195-024-01666-7.
58. Deryusheva, E.I.; Shevelyova, M.P.; Rastrygina, V.A.; Nemashkalova, E.L.; Vologzhannikova, A.A.; Machulin, A.V.; Nazipova, A.A.; Permyakova, M.E.; Permyakov, S.E.; Litus, E.A. In Search for Low-Molecular-Weight Ligands of Human Serum Albumin That Affect Its Affinity for Monomeric Amyloid beta Peptide. *Int J Mol Sci* **2024**, *25*, doi:ijms25094975 [pii]ijms-25-04975 [pii]10.3390/ijms25094975.
59. Kamynina, A.V.; Esteras, N.; Koroiev, D.O.; Bobkova, N.V.; Balasanyants, S.M.; Simonyan, R.A.; Avetisyan, A.V.; Abramov, A.Y.; Volpina, O.M. Synthetic Fragments of Receptor for Advanced Glycation End Products Bind Beta-Amyloid 1–40 and Protect Primary Brain Cells From Beta-Amyloid Toxicity. *Frontiers in Neuroscience* **2018**, *12*, doi:10.3389/fnins.2018.00681.
60. Lv, J.; Pan, Y.; Li, X.; Cheng, D.; Liu, S.; Shi, H.; Zhang, Y. The Imaging of Insulinomas Using a Radionuclide-Labelled Molecule of the GLP-1 Analogue Liraglutide: A New Application of Liraglutide. *PloS one* **2014**, *9*, e96833, doi:10.1371/journal.pone.0096833.

61. Jacobsen, L.V.; Flint, A.; Olsen, A.K.; Ingwersen, S.H. Liraglutide in Type 2 Diabetes Mellitus: Clinical Pharmacokinetics and Pharmacodynamics. *Clinical pharmacokinetics* **2016**, *55*, 657-672, doi:10.1007/s40262-015-0343-6.
62. Yang, X.D.; Yang, Y.Y. Clinical Pharmacokinetics of Semaglutide: A Systematic Review. *Drug design, development and therapy* **2024**, *18*, 2555-2570, doi:10.2147/dddt.s470826.
63. Mehta, P.D.; Pirttila, T.; Mehta, S.P.; Sersen, E.A.; Aisen, P.S.; Wisniewski, H.M. Plasma and cerebrospinal fluid levels of amyloid beta proteins 1-40 and 1-42 in Alzheimer disease. *Archives of neurology* **2000**, *57*, 100-105, doi:10.1001/archneur.57.1.100.
64. Zapadka, K.L.; Becher, F.J.; Uddin, S.; Varley, P.G.; Bishop, S.; Gomes Dos Santos, A.L.; Jackson, S.E. A pH-Induced Switch in Human Glucagon-like Peptide-1 Aggregation Kinetics. *J Am Chem Soc* **2016**, *138*, 16259-16265, doi:10.1021/jacs.6b05025.
65. Prada Brichtova, E.; Krupova, M.; Bour, P.; Lindo, V.; Gomes Dos Santos, A.; Jackson, S.E. Glucagon-like peptide 1 aggregates into low-molecular-weight oligomers off-pathway to fibrillation. *Biophys J* **2023**, *122*, 2475-2488, doi:S0006-3495(23)00298-9 [pii]10.1016/j.bpj.2023.04.027.
66. Wang, K.; Chen, K. Direct Assessment of Oligomerization of Chemically Modified Peptides and Proteins in Formulations using DLS and DOSY-NMR. *Pharm Res* **2023**, *40*, 1329-1339, doi:10.1007/s11095-022-03468-8 [pii]10.1007/s11095-022-03468-8.
67. Venanzi, M.; Savioli, M.; Cimino, R.; Gatto, E.; Palleschi, A.; Ripani, G.; Cicero, D.; Placidi, E.; Orvieto, F.; Bianchi, E. A spectroscopic and molecular dynamics study on the aggregation process of a long-acting lipidated therapeutic peptide: the case of semaglutide. *Soft Matter* **2020**, *16*, 10122-10131, doi:10.1039/d0sm01011a.
68. Wang, Y.; Lomakin, A.; Kanai, S.; Alex, R.; Benedek, G.B. Transformation of oligomers of lipidated peptide induced by change in pH. *Mol Pharm* **2015**, *12*, 411-419, doi:10.1021/mp500519s.
69. Wolff, M.; Gast, K.; Evers, A.; Kurz, M.; Pfeiffer-Marek, S.; Schuler, A.; Seckler, R.; Thalhammer, A. A Conserved Hydrophobic Moiety and Helix-Helix Interactions Drive the Self-Assembly of the Incretin Analog Exendin-4. *Biomolecules* **2021**, *11*, doi:biom11091305 [pii]biomolecules-11-01305 [pii]10.3390/biom11091305.
70. Calanna, S.; Christensen, M.; Holst, J.; Laferrère, B.; Gluud, L.; Vilsbøll, T.; Knop, F. Secretion of Glucagon-Like Peptide-1 in Patients With Type 2 Diabetes Mellitus - Systematic Review and Meta-Analysis of Clinical Studies. *Diabetologia* **2013**, *56*, doi:10.1007/s00125-013-2841-0.
71. Balks, H.J.; Holst, J.J.; von zur Mühlen, A.; Brabant, G. Rapid Oscillations in Plasma Glucagon-Like Peptide-1 (GLP-1) in Humans: Cholinergic Control of GLP-1 Secretion via Muscarinic Receptors1. *The Journal of Clinical Endocrinology & Metabolism* **1997**, *82*, 786-790, doi:10.1210/jcem.82.3.3816.
72. Fineman, M.; Flanagan, S.; Taylor, K.; Aisporna, M.; Shen, L.Z.; Mace, K.F.; Walsh, B.; Diamant, M.; Cirincione, B.; Kothare, P.; et al. Pharmacokinetics and Pharmacodynamics of Exenatide Extended-Release After Single and Multiple Dosing. *Clinical pharmacokinetics* **2011**, *50*, 65-74, doi:10.2165/11585880-000000000-00000.
73. Kastin, A.J.; Akerstrom, V. Entry of exendin-4 into brain is rapid but may be limited at high doses. *International journal of obesity and related metabolic disorders : journal of the International Association for the Study of Obesity* **2003**, *27*, 313-318, doi:10.1038/sj.ijo.0802206.
74. Gabery, S.; Salinas, C.G.; Paulsen, S.J.; Ahnfelt-Rønne, J.; Alanentalo, T.; Baquero, A.F.; Buckley, S.T.; Farkas, E.; Fekete, C.; Frederiksen, K.S.; et al. Semaglutide lowers body weight in rodents via distributed neural pathways. *JCI insight* **2020**, *5*, doi:10.1172/jci.insight.133429.
75. Lovshin, J.A.; Drucker, D.J. Incretin-based therapies for type 2 diabetes mellitus. *Nature Reviews Endocrinology* **2009**, *5*, 262-269, doi:10.1038/nrendo.2009.48.
76. Dejgaard, T.; Frandsen, C.; Kielgast, U.; Størling, J.; Overgaard, A.; Svane, M.; Olsen, M.H.; Thorsteinsson, B.; Andersen, H.; Krarup, T.; et al. Liraglutide enhances insulin secretion and prolongs the remission period in adults with newly diagnosed type 1 diabetes (the NewLira study): A randomized, double-blind, placebo-controlled trial. *Diabetes, obesity & metabolism* **2024**, *26*, doi:10.1111/dom.15889.

77. Zheng, Z.; Zong, Y.; Ma, Y.; Tian, Y.; Pang, Y.; Zhang, C.; Gao, J. Glucagon-like peptide-1 receptor: mechanisms and advances in therapy. *Signal Transduction and Targeted Therapy* **2024**, *9*, 234, doi:10.1038/s41392-024-01931-z.
78. Desta, I.T.; Porter, K.A.; Xia, B.; Kozakov, D.; Vajda, S. Performance and Its Limits in Rigid Body Protein-Protein Docking. *Structure* **2020**, *28*, 1071-1081 e1073, doi:S0969-2126(20)30209-4 [pii]10.1016/j.str.2020.06.006.
79. Jarero-Basulto, J.J.; Gasca-Martínez, Y.; Rivera-Cervantes, M.C.; Gasca-Martínez, D.; Carrillo-González, N.J.; Beas-Zárate, C.; Gudiño-Cabrera, G. Cytotoxic Effect of Amyloid- β 1-42 Oligomers on Endoplasmic Reticulum and Golgi Apparatus Arrangement in SH-SY5Y Neuroblastoma Cells. *NeuroSci* **2024**, *5*, 141-157, doi:10.3390/neurosci5020010.
80. Vander Zanden, C.M.; Chi, E.Y. Passive Immunotherapies Targeting Amyloid Beta and Tau Oligomers in Alzheimer's Disease. *Journal of pharmaceutical sciences* **2020**, *109*, 68-73, doi:10.1016/j.xphs.2019.10.024.
81. Chang, Y.F.; Zhang, D.; Hu, W.M.; Liu, D.X.; Li, L. Semaglutide-mediated protection against A β correlated with enhancement of autophagy and inhibition of apoptosis. *J Clin Neurosci* **2020**, *81*, 234-239, doi:10.1016/j.jocn.2020.09.054.
82. Liu, X.Y.; Wang, L.X.; Chen, Z.; Liu, L.B. Liraglutide prevents beta-amyloid-induced neurotoxicity in SH-SY5Y cells via a PI3K-dependent signaling pathway. *Neurological research* **2016**, *38*, 313-319, doi:10.1080/01616412.2016.1145914.
83. Litus, E.A.; Kazakov, A.S.; Deryusheva, E.I.; Nemashkalova, E.L.; Shevelyova, M.P.; Machulin, A.V.; Nazipova, A.A.; Permyakova, M.E.; Uversky, V.N.; Permyakov, S.E. Ibuprofen Favors Binding of Amyloid-beta Peptide to Its Depot, Serum Albumin. *Int J Mol Sci* **2022**, *23*, doi:ijms23116168 [pii]ijms-23-06168 [pii]10.3390/ijms23116168.
84. Catanzariti, A.M.; Soboleva, T.A.; Jans, D.A.; Board, P.G.; Baker, R.T. An efficient system for high-level expression and easy purification of authentic recombinant proteins. *Protein Sci* **2004**, *13*, 1331-1339, doi:13/5/1331 [pii]0131331 [pii]10.1110/ps.04618904.
85. Pace, C.N.; Vajdos, F.; Fee, L.; Grimsley, G.; Gray, T. How to measure and predict the molar absorption coefficient of a protein. *Protein Sci* **1995**, *4*, 2411-2423, doi:10.1002/pro.5560041120.
86. De Ferrari, G.V.; Mallender, W.D.; Inestrosa, N.C.; Rosenberry, T.L. Thioflavin T is a fluorescent probe of the acetylcholinesterase peripheral site that reveals conformational interactions between the peripheral and acylation sites. *J Biol Chem* **2001**, *276*, 23282-23287, doi:S0021-9258(20)78313-4 [pii]10.1074/jbc.M009596200.
87. Deryusheva, E.I.; Shevelyova, M.P.; Rastrygina, V.A.; Nemashkalova, E.L.; Vologzhannikova, A.A.; Machulin, A.V.; Nazipova, A.A.; Permyakova, M.E.; Permyakov, S.E.; Litus, E.A. In Search for Low-Molecular-Weight Ligands of Human Serum Albumin That Affect Its Affinity for Monomeric Amyloid β Peptide. *Int J Mol Sci* **2024**, *25*, doi:10.3390/ijms25094975.
88. Uversky, V.N. Natively unfolded proteins: a point where biology waits for physics. *Protein Sci* **2002**, *11*, 739-756, doi:0110739 [pii]10.1110/ps.4210102.
89. Berman, H.M.; Burley, S.K. Protein Data Bank (PDB): Fifty-three years young and having a transformative impact on science and society. *Quarterly reviews of biophysics* **2025**, *58*, e9, doi:10.1017/s0033583525000034.

Disclaimer/Publisher's Note: The statements, opinions and data contained in all publications are solely those of the individual author(s) and contributor(s) and not of MDPI and/or the editor(s). MDPI and/or the editor(s) disclaim responsibility for any injury to people or property resulting from any ideas, methods, instructions or products referred to in the content.